PAK4 promotes kinase-independent stabilization of RhoU to modulate cell adhesion

Anna E. Dart,[1] Gary M. Box,[2] William Court,[2] Madeline E. Gale,[1] John P. Brown,[3] Sarah E. Pinder,[3] Suzanne A. Eccles,[2] and Claire M. Wells[1]

[1]Division of Cancer Studies, King's College London, London SE1 1UL, England, UK
[2]Tumour Biology and Metastasis, Cancer Research UK Cancer Therapeutics Unit, The Institute of Cancer Research, London SM2 5NG, England, UK
[3]Breast Research Pathology, Department of Research Oncology, Division of Cancer Studies, School of Medicine, Guy's Hospital, King's College London, London SE1 9RT, England, UK

P21-activated kinase 4 (PAK4) is a Cdc42 effector protein thought to regulate cell adhesion disassembly in a kinase-dependent manner. We found that PAK4 expression is significantly higher in high-grade human breast cancer patient samples, whereas depletion of PAK4 modifies cell adhesion dynamics of breast cancer cells. Surprisingly, systematic analysis of PAK4 functionality revealed that PAK4-driven adhesion turnover is neither dependent on Cdc42 binding nor kinase activity. Rather, reduced expression of PAK4 leads to a concomitant loss of RhoU expression. We report that RhoU is targeted for ubiquitination by the Rab40A–Cullin 5 complex and demonstrate that PAK4 protects RhoU from ubiquitination in a kinase-independent manner. Overexpression of RhoU rescues the PAK4 depletion phenotype, whereas loss of RhoU expression reduces cell adhesion turnover and migration. These data support a new kinase-independent mechanism for PAK4 function, where an important role of PAK4 in cellular adhesions is to stabilize RhoU protein levels. Thus, PAK4 and RhoU cooperate to drive adhesion turnover and promote cell migration.

Introduction

P21-activated kinase (PAK) function impacts a plethora of cellular processes, including cell migration, cell survival, embryonic development, and transcriptional regulation (Qu et al., 2003; Li and Minden, 2005; Bompard et al., 2010; Li et al., 2012). Indeed, there is much pharmaceutical and academic interest in developing PAK-specific inhibitors (Murray et al., 2010; Zhang et al., 2012).

PAKs are serine/threonine kinases best known as Rac and Cdc42 effector proteins. The mammalian family of PAK proteins is subdivided into two groups: group I PAKs (PAK1–3) and group II PAKs (PAK4–6; Dart and Wells, 2013). Functionally, group II PAKs are thought to preferentially interact with Cdc42 and related Rho family small GTPases (Abo et al., 1998; Wu and Frost, 2006; Shepelev and Korobko, 2012). However, although interaction with GTPases can lead to increased group I PAK activation (Eswaran et al., 2008), the part played by the Rho GTPases in activating group II PAKs has been the subject of much debate (Baskaran et al., 2012; Ha et al., 2012; Wang et al., 2013), and the role of other Cdc42-related family members has not been elucidated.

Of the group II PAKs, PAK4 has been specifically associated with several features of tumorigenesis, such as anchorage-independent growth, increased cell survival, migration, and invasion (Gnesutta et al., 2001; Callow et al., 2002; Siu et al., 2010; Rafn et al., 2012; Park et al., 2013; Tabusa et al., 2013). There is a strong correlation between PAK4 and breast cancer; PAK4 is up-regulated at the protein level in several breast cancer cell lines in addition to primary human breast and rat mammary tumor samples (Callow et al., 2002; Liu et al., 2008, 2010). Furthermore, the chromosomal region 19q13.2, in which PAK4 resides, is often amplified at a high frequency in aggressive breast cancers with basal-like features (Yu et al., 2009).

Most known PAK4 functions depend on kinase activity, and so far, kinase-independent events have not been associated with cell adhesion and migration (Dart and Wells, 2013). Moreover, a mechanistic basis of PAK4 function within breast cancer cells remains to be elucidated. It had been previously established in prostate cancer that PAK4 was essential for cell migration via phosphorylation of LIMK1 in mesenchymal-like cells (Ahmed et al., 2008; Whale et al., 2013), but no functional link to cell adhesion dynamics was reported. In contrast, in colony-forming cells, PAK4 promoted the disassembly of focal adhesions via phosphorylation of paxillin at serine 272 (S272; Wells et al., 2010).

Although the molecular processes that drive focal adhesion formation have been extensively characterized, the process of adhesion disassembly is less well defined (Wehrle-Haller, 2012). However, disassembly is likely to involve spatiotempo-

Correspondence to Claire M. Wells: claire.wells@kcl.ac.uk

Abbreviations used in this paper: ECS, Elongin–Cullin–SOCS box; GBD, GTPase-binding domain; GEF, guanine nucleotide exchange factor; PAK, P21-activated kinase; Ub, ubiquitin; WT, wild type.

The Rockefeller University Press $30.00
J. Cell Biol. Vol. 211 No. 4 863–879
www.jcb.org/cgi/doi/10.1083/jcb.201501072

ral regulation of the Rho family GTPases. Interestingly, RhoU is thought to modulate focal adhesion dynamics in HeLa cells (Chuang et al., 2007; Ory et al., 2007). Unlike conventional GTPases, RhoU exhibits extremely high intrinsic guanine nucleotide exchange activity and is rendered largely in the GTP-loaded conformation. Thus, regulation of RhoU activity is thought to be distinct from that of conventional Rho GTPases (Saras et al., 2004; Shutes et al., 2004).

Results

PAK4 expression is correlated with breast cancer cell migration

Recent studies have suggested that PAK4 expression may be indicative of a poorer prognosis in cancer (Siu et al., 2010; Zhang et al., 2011). We examined the expression level of PAK4 in 300 human breast cancer tissue samples with normal controls. Both weak and strong cytoplasmic PAK4 staining of epithelial cells was observed (Fig. 1 A). Importantly, a significantly higher level of PAK4 expression was found in the more severe grade of invasive breast carcinomas (Fig. 1 A). To further examine the role of PAK4 in breast cancer, we generated stable MDA-MB-231 cell lines expressing control nontargeting or one of two independent *PAK4*-specific shRNA. PAK4 protein levels were reduced by >50% in the cell lines stably expressing *PAK4* shRNA (Oligo1 and Oligo3) without detectably changing the levels of the group I PAK, PAK1, and another group II PAK, PAK6 (Fig. 1 B), or phospho-PAK6 (S560) levels (Fig. 1 B). Loss of PAK4 expression correlated with an increase in the adhesion of MDA-MB-231 cells to a fibronectin substratum (Fig. 1 C) with a concomitant increase in the number and length of focal adhesions compared with control cells (Fig. 1 D), a phenotype replicated in MCF-7 cells (Fig. S1, A–C). In contrast, depletion of PAK1/PAK2 expression (Fig. S1 D) did not phenocopy the PAK4-depleted cells (Fig. S1 E). Indeed, reduced expression of either protein had no effect on focal adhesion number (Fig. S1 E). Thus, in breast cancer cells, the PAK4 adhesion phenotype dominates (Wells et al., 2010). We have previously shown using interference reflection microscopy that this PAK4-mediated change in adhesion dynamics is a direct consequence of reduced cell substratum adhesion disassembly (Wells et al., 2010). In breast cancer cells, we were also able to detect endogenous PAK4 in a complex with paxillin and vinculin (Fig. S2 A). Control of cellular adhesion is frequently related to cell migration, and we found that knockdown of PAK4 significantly attenuated migration potential (MDA-MB-231 [Fig. 1 E] and MCF-7 [Fig. S1 F]), demonstrating that PAK4 expression is necessary for optimal breast cancer cell motility.

PAK4-dependent cell adhesion does not require Cdc42

Our data clearly demonstrate that PAK4 drives breast cancer cell migration. However, a requirement for kinase activity and regulation of PAK4 activity remains to be defined. PAK4 preferentially binds to GTP-bound Cdc42 (Abo et al., 1998), which can activate PAK4 (Baskaran et al., 2012). Moreover, Cdc42 binding is necessary for full hepatocyte growth factor–mediated motility of PC3 prostate cancer cells (Whale et al., 2013). Yet, both PAK4r (shRNA-resistant PAK4; Whale et al., 2013) and PAK4 (H19, 22L)r (a Cdc42 binding–deficient mutant; Whale et al., 2013) were able to rescue the adhesion of PAK4 knockdown cells to control levels (Fig. 2, A and B), demonstrating that an interaction between Cdc42 and PAK4 is not required. We therefore sought to identify whether another Rho GTPase might regulate PAK4 function. PAK4 did not bind to Rac1, RhoG, RhoA, RhoJ, or RhoQ (Fig. S2 B). As expected, PAK4 bound to Cdc42 but also interacted with RhoU (Fig. 2 C) and RhoV (Fig. S2 B). Because RhoU has already been shown to localize to focal adhesions (Chuang et al., 2007; Ory et al., 2007), we chose to focus our attention on this particular small GTPase. RhoU interacted with full-length recombinant PAK4, the Δkinase domain, and, more specifically, the GTPase-binding domain (GBD; Fig. 2 D). We next performed the reverse set of experiments to determine which domain of RhoU (Fig. 2 E) bound to PAK4. We observed binding between PAK4 and both the ΔN- and ΔC-terminal mutants of RhoU, so we can therefore deduce that the region between these two termini, containing the effector and GTPase domains, most likely contributes to the interaction (Fig. 2 E).

Both Cdc42 and RhoU can interact with the GBD of PAK4, but we found that PAK4 (H19, 22L) can still bind to RhoU (Fig. 2 F) and indeed rescue the adhesion phenotype (Fig. 2 B). This result supports the notion that the critical residues necessary for binding within the PAK4 GBD differs depending on the GTPase species engaged. It is well established that RhoU can bind to and activate PAK1 (Tao et al., 2001). In cells coexpressing similar amounts of GFP-PAK1 and HA-PAK4, we found that RhoU could still bind to either PAK1 or PAK4 to a similar level in the presence of the other (Fig. S2 C); although there was a suggestion of a preference for PAK4, it was not statistically significant. Because neither PAK1 nor PAK4 could completely out-compete one another for binding to RhoU, we reasoned that the residues important within the RhoU effector domain crucial for interaction with PAK1 might differ from those of PAK4. PAK1 cannot bind to the RhoU 3M mutant (Ory et al., 2007), but we found that PAK4 was able to bind to it (Fig. S2, D and E). Thus, differential binding between the RhoU and PAK family proteins could account for the diverse biological functions of RhoU.

The interaction between RhoU and PAK4 is kinase independent

Because RhoU is closely related to Cdc42, we speculated that RhoU might regulate PAK4 activity during adhesion dynamics, especially given that Cdc42 binding is not required (Fig. 2 B). Autophosphorylation of PAK4 at S474 is thought to be a marker of kinase activity (Wells et al., 2010), but unlike that of group I PAKs, this autophosphorylation is not believed to entirely be a result of Rho GTPase binding (Baskaran et al., 2012; Ha et al., 2012). We found that phospho-PAK4 (S474) levels were unchanged in the presence of overexpressed RhoU (Fig. 3 A). Furthermore, RhoU was not identified as a substrate of PAK4 (Fig. 3 B) and moreover, autophosphorylation of PAK4 and histone H1 substrate phosphorylation were not enhanced by the presence of RhoU (compare Fig. S2 F with Fig. 3 B). Therefore, it is likely that any functional outcome of the interaction between RhoU and PAK4 would be via a kinase-independent mechanism. RhoU is an atypical GTPase whose activity is more likely to be regulated by expression level or posttranslational modifications (Tao et al., 2001; Saras et al., 2004; Shutes et al., 2004). Given that RhoU does not activate PAK4 and RhoU was not a PAK4 substrate, we considered whether PAK4 might regulate RhoU expression. Interestingly, we found that depletion of

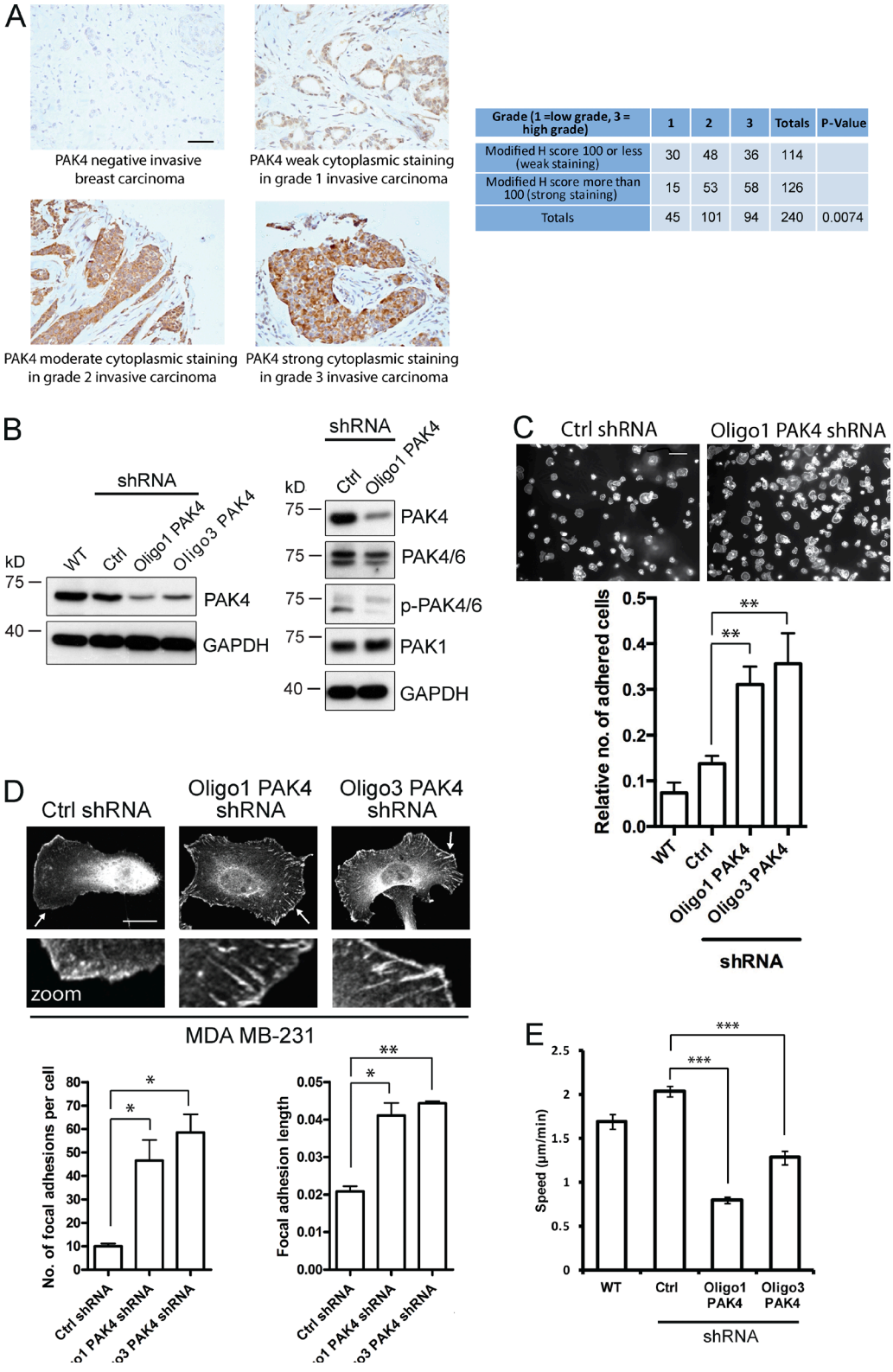

Grade (1 =low grade, 3 = high grade)	1	2	3	Totals	P-Value
Modified H score 100 or less (weak staining)	30	48	36	114	
Modified H score more than 100 (strong staining)	15	53	58	126	
Totals	45	101	94	240	0.0074

Figure 1. **Reduced PAK4 expression leads to an increase in MDA-MB-231 cell adhesion.** (A, left) Immunohistochemical staining of human breast cancer tissues. Samples stained for PAK4 (brown) using an in-house PAK4-specific antibody and counterstained hematoxylin (blue) to reveal cellular structure. Bar, 50 μm. (Right) Observed frequencies for modified H scores of PAK4 staining in human breast cancer tissue microarray. Modified H scores were generated by multiplying intensity (scored between 0 and 300) and percentage of cytoplasmic staining. χ^2 p-values calculated for H scores associated with cancer grade. (B) WT, control, and PAK4 (Oligo1 and Oligo3) shRNA-expressing stable MDA-MB-231 cell lysates blotted with an in-house PAK4 antibody. GAP DH was used as a loading control. Control and PAK4 (Oligo1) shRNA-expressing MDA-MB-231 cell lysates also blotted for PAK4/6, phospho-PAK4/6, and PAK1. (C, top) F-actin staining of control and PAK4 shRNA-expressing MDA-MB-231 cells plated onto 10 μg/ml fibronectin and fixed after 60 min. Bar, 100 μm. (Bottom) Adhesion assay of WT, control, and PAK4 shRNA-expressing MDA-MB-231 cells plated onto 10 μg/ml fibronectin for 60 min. Relative number

PAK4 from MDA-MB-231 cells correlated with a loss of RhoU expression (Fig. 3 C), which could be replicated in MCF-7 cells (Fig. S1 G). Conversely, when we overexpressed PAK4 in MDA-MB-231 cells, an increase in endogenous RhoU protein expression was observed (Fig. S2 G). However, the mRNA expression of RhoU was not significantly unaltered in PAK4 knockdown cells when compared with control cells, suggesting that PAK4 regulation of RhoU expression levels occurs post-transcriptionally (Fig. 3 D), possibly via ubiquitination.

RhoU is ubiquitinated

Recently, it has been recognized that small GTPases, such as RhoA and Rac1, can be ubiquitinated as an alternative pathway to terminate signaling (Nethe and Hordijk, 2010). However, ubiquitination of RhoU had not been previously reported. We now find that RhoU can form RhoU–ubiquitin (Ub) conjugates (Fig. 3 E; HA-RhoU(Ub)n, visualized as multiple HA-positive bands that increase in size as RhoU–Ub levels are increased, rendering a gel smear; Rolli-Derkinderen et al., 2005; Visvikis et al., 2008). This shift in molecular weight is entirely consistent with increased ubiquitination (Rolli-Derkinderen et al., 2005; Visvikis et al., 2008). The linkage specificity of ubiquitination can determine the stability of the target protein, where K48-linked ubiquitination targets substrates for proteasomal degradation, whereas K63-linked ubiquitination serves as a regulatory signal (Weissman, 2001). We next sought to confirm RhoU ubiquitination topologies. We used HA-tagged wild-type (WT) Ub and K48R and K63R Ub mutants, in which single lysine to arginine mutations at positions 48 and 63 are expected to disrupt Ub chain assembly. The mutation of K48 in Ub abolished RhoU ubiquitination, whereas the K63 mutation only moderately decreased the formation of RhoU–Ub conjugates (Fig. 3 E). This preferential K48-linked ubiquitination of RhoU is in line with a phenotype of RhoU degradation. Having confirmed that RhoU is targeted for ubiquitination, we next sought to identify the specific sites for Ub addition. Recent large-scale ubiquitome studies exploiting a combination of diglycine antibodies, proteomics, and mass spectrometry have identified numerous in vivo ubiquitination sites (Kessler, 2013). Interestingly, one such study suggested that mouse RhoU has two putative ubiquitination sites, equivalent to K177 and K248 in human RhoU (Wagner et al., 2012). Initially, we performed individual substitutions of the eight lysines present in the C-terminal sequence of RhoU to arginine and analyzed the mutated proteins using the Ub co-immunoprecipitation assay. Of the eight lysines tested, only the RhoU K248R point mutant notably decreased the ubiquitination of RhoU (not depicted and Fig. 3 F), consistent with the previous predictions (Wagner et al., 2012). However, we observed that the RhoU ubiquitination signal was not completely lost in the RhoU K248R mutant. Thus, we reasoned the second predicted site (Wagner et al., 2012) on RhoU might also be ubiquitinated. Indeed, it is common for proteins to have more than one ubiquitinated lysine (Rodriguez et al., 2000). Consequently, we produced a K to R point mutant of RhoU at position 177 as well as a double point mutant at positions 177 and 248. The single RhoU K177R point mutant similarly reduced the ubiquitination of RhoU, and the double mutant RhoU K177, 248R also strongly impaired RhoU–Ub conjugate formation (Fig. 3 F). As a result, we propose that the major sites of ubiquitination in RhoU are lysines 177 and 248.

E3 Ub ligase Rab40A targets RhoU for ubiquitination

Ubiquitination of a protein is catalyzed by three enzymatic steps driven by a trio of enzymes, E1, E2, and E3, which in turn activate and deliver the Ub molecules to the targeted substrate. The last step of this process, whereby Ub is covalently attached to lysine residues within the target protein, is performed by an E3 Ub ligase (Nethe and Hordijk, 2010). We have used a high-throughput protein-binding microarray approach to screen a CDI HuProt microarray comprising of nearly 20,000 human full-length proteins for binding to RhoU, with specific emphasis on E3 ligases. Under rigorous and conservative criteria described in the supplementals, 121 proteins were identified as RhoU-interacting proteins (Table S1), showing statistical significance ($P < 0.05$) and a positive M_L value indicative of an increase in signal after RhoU treatment compared with control buffer alone. From this screen, we identified Rab40A, a Rab GTPase, as a binding partner for RhoU (Fig. 4 A). Human Rab40A is believed to be the substrate recognition/binding component of an SCF-like ECS (Elongin–Cullin–SOCS box protein) E3 Ub ligase complex by virtue of its homology to that of the *Xenopus*-protein, which interacts with ElonginB/C and Cullin 5 to form a Ub ligase (Lee et al., 2007). GST pull-down analyses validated Rab40A as a RhoU-interacting protein and demonstrated that Cullin 5 can also form a complex with RhoU (Fig. 4 B).

To test whether Rab40A, via its Ub ligase activity, could indeed modulate RhoU stability, we overexpressed Rab40A and observed the level of endogenous RhoU. Rab40A overexpression consistently resulted in reduced RhoU levels, and, moreover, coexpression of Rab40A and Cullin 5 further decreased RhoU protein (Fig. 4 C). In addition, an inactivated Cullin 5 mutant (Cul5 K799R; Teckchandani et al., 2014) was unable to modulate RhoU levels (Fig. 4 C). Consistent with the involvement of Rab40A and Cullin 5 in the down-regulation of RhoU, overexpression of the E3 Ub ligase complex promoted the ubiquitination of RhoU (Fig. 4 D). These data support a role for the recruitment of RhoU by Rab40A to an ECS complex whereby it becomes ubiquitinated.

PAK4 protects RhoU from ubiquitination

Having confirmed that RhoU can be ubiquitinated and that ubiquitination can be delivered via a Rab40A complex, we reasoned that reducing Rab40A expression in PAK4-depleted cells would promote RhoU reexpression. Interestingly, though we did find that RhoU levels recovered (Fig. 4 E), we could not recover them to control levels. Thus, RhoU might be targeted by more than one E3 Ub ligase. Sharpin (SHANK-associated RH domain–interacting protein), part of an E3 ligase complex, has been linked to adhesion dynamics (Rantala et al., 2011) and

of adhered cells is absorbance at 560 nm. **, $P < 0.01$. (D) Paxillin labeling of MDA-MB-231 cells stably expressing control or PAK4 shRNA. Arrows highlight the area in magnified insets. Bar, 20 µm. The mean number of focal adhesions per cell and the mean length of focal adhesions for all cell populations were measured using ImageJ software. $n > 60$ cells per condition over three independent experiments. *, $P < 0.05$; **, $P < 0.01$. (E) WT, control, and PAK4 knockdown MDA-MB-231 cells plated onto 10 µg/ml fibronectin were filmed for 18 h with time-lapse video microscopy. *n*, 60 individual cells per condition tracked over three separate experiments. The mean migration speed ± SEM were calculated for each condition. ***, $P < 0.001$. Ctrl, control.

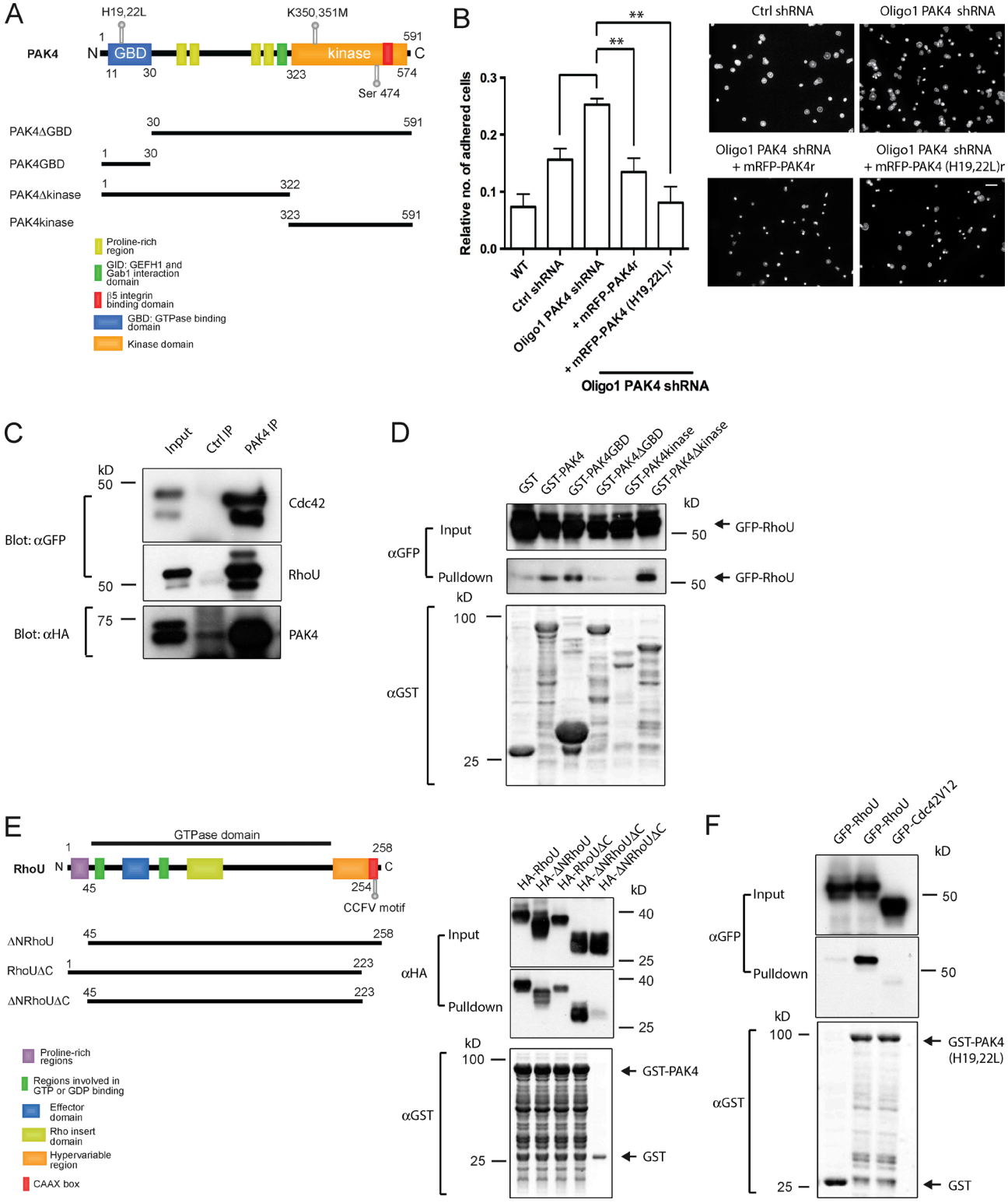

Figure 2. **PAK4 interacts with RhoU.** (A) Schematic of PAK4 domain structure with N-terminal GBD and a C-terminal kinase domain. (B, left) Adhesion assay of Oligo1 PAK4-depleted MDA-MB-231 cells expressing shRNA-resistant mRFP-PAK4 derivatives plated onto 10 µg/ml fibronectin for 60 min. Relative number of adhered cells is absorbance at 560 nm. Error bars represent mean ± SEM. **, $P < 0.01$. (Right) F-actin staining of same cell conditions plated onto 10 µg/ml fibronectin and fixed after 60 min. Bar, 100 µm. (C) Anti–in-house PAK4 antibody coimmunoprecipitation of Cdc42 and RhoU from HEK-293 cells expressing HA-PAK4 and GFP-Cdc42 or GFP-RhoU. The control immunoprecipitation was rabbit anti-VSV-G antibody. (D) Purified GST, GST-PAK4, GST-PAK4 GBD, GST-PAK4 ΔGBD, GST-PAK4 kinase domain, and GST-PAK4 Δkinase domain beads were used to pull down GFP-RhoU from MDA-MB-231 cell lysates. Samples were analyzed by anti-GFP immunoblotting and Coomassie staining. Representative of three separate experiments. (E) Schematic of RhoU domain structure comprising of N-terminal proline-rich regions, a GTPase domain, and a C-terminal CAAX box motif. GST-PAK4 beads

was highlighted in our screen on the periphery of significance (Fig. 4 A). We find that Sharpin overexpression is also able to decrease endogenous RhoU levels (Fig. S2 H), suggesting that regulation of RhoU protein levels via ubiquitination is likely to be a complex spatial–temporal process.

The recovery of RhoU expression in cells codepleted of Rab40A and PAK4 strongly suggests that PAK4 plays an active part in protecting RhoU from degradation. Thus, we next tested whether PAK4 could directly protect RhoU from ubiquitination. We found that the prominence of RhoU–Ub conjugates was dramatically decreased in the presence of GFP-PAK4 (loss of multiple HA-positive bands; Fig. 4, F and G). This result provides clear evidence that PAK4 protects RhoU from Ub-mediated protein degradation. The N-terminal extension of RhoU is thought to display an autoinhibitory function via binding to the GTPase domain of RhoU (Shutes et al., 2004). We found that the N-terminal deletion mutant of RhoU (Fig. 4 F), which still binds to PAK4 (Fig. 2 E), was heavily ubiquitinated, and importantly, this was also protected by coexpression of PAK4 (Fig. 4 F). In contrast, deletion of the C-terminal residues including K248 (Fig. 3 F) almost completely abolished the ubiquitination of RhoU (Fig. 4 F), and this was not impacted by PAK4 overexpression. Importantly, we observed that both the kinase-dead and the Cdc42 binding–deficient mutants of PAK4, but not PAK4ΔGBD, were as equally competent as full-length PAK4 in reducing the amount of RhoU–Ub conjugates (Fig. 4 G). In combination, these data demonstrate that the interaction between RhoU and PAK4 is both sufficient and crucial for protecting RhoU from ubiquitination, but does not require PAK4 kinase activity.

RhoU expression can rescue PAK4 knockdown phenotypes

Our data point to an interaction between PAK4 and RhoU that is kinase independent but when disrupted (by reduction of PAK4 expression) leads to a loss of RhoU expression via ubiquitination. Given that RhoU expression has also been linked with adhesion disassembly in other cell types (Chuang et al., 2007; Ory et al., 2007; Bhavsar et al., 2013), we speculated that the PAK4 knockdown adhesion phenotype could be rescued by exogenous expression to restore RhoU to at least control levels. Strikingly, GFP-RhoU was able to rescue the phenotype of PAK4-depleted cells (Fig. 5 A). Furthermore, a PAK4 kinase-dead mutant (K350, 351M)r also significantly reduced adhesion compared with PAK4 knockdown cells (Fig. 5 A). RhoU rescues the augmented adhesion of PAK4 knockdown cells through a change in focal adhesion dynamics in the same manner as PAK4r expression (Fig. 5 B). Equally, the RhoU effector loop mutants (including RhoU 3M) were also able to alter the adhesion properties of PAK4-depleted cells by significantly decreasing both the number and length of focal adhesions (Fig. S3, A and B), demonstrating that PAK1 is not likely to be required for RhoU-mediated disassembly of focal adhesions. Importantly, expression of PAK4r, both the PAK4 mutants PAK4 (H19, 22L)r and PAK4 (K350, 351M)r, and RhoU was able to rescue the mean speed of cell motility in PAK4 knockdown cells (MDA-MB-231 [Fig. 5 C] and MCF-7 [Fig. S1 F]), overall emphasizing a kinase-independent function for PAK4 in adhesion and migration upstream of RhoU and not requiring Cdc42 interaction.

Our data indicate a role for a PAK4–RhoU complex in focal adhesion disassembly. However, in some T cell lines, RhoU expression promotes adhesion (Bhavsar et al., 2013). Thus, we sought to define the precise involvement of RhoU in the regulation of focal adhesion disassembly in MDA-MB-231 cells. Loss of RhoU expression significantly increased the cellular adhesion, which could be rescued by the overexpression of RhoUr, a protein resistant to RNAi (Fig. 6, A and B). Moreover, we found significant differences in the number of focal adhesions (Fig. 6 C). This phenocopy of PAK4 knockdown has also been observed with knockdown of RhoU in both HeLa and NIH 3T3 cells (Chuang et al., 2007; Ory et al., 2007). Furthermore, mean cell migration speed was significantly decreased in RhoU shRNA-expressing cells (MDA-MB-231 [Fig. 6 D] and MCF-7 [Fig. S1 F]). Because of technical limitations of available antibodies, we were unable to localize endogenous RhoU, and GFP-RhoU overexpression routinely led to cell rounding, a consequence of enhanced adhesion disassembly that we have previously noted (Wells et al., 2002). However, on the rare occasion where we could image GFP-RhoU, we were able to see localization in adhesions (Fig. S3 C). Thus, in MDA-MB-231 cells, RhoU is more closely associated with adhesion disassembly than formation and appears to function downstream of PAK4 in mediating adhesion disassembly.

RhoU promotes paxillin S272 phosphorylation

Our previous work and others had demonstrated that PAK4-driven phosphorylation of paxillin S272 is an essential step in cell adhesion turnover (Nayal et al., 2006; Wells et al., 2010). Indeed, we again find that PAK4-depleted MDA-MB-231 cells exhibit reduced levels of paxillin S272 phosphorylation (Fig. 7 A), whereas reduction of PAK1 levels in MDA-MB-231 cells by siRNA did not concomitantly decrease paxillin S272 levels (Fig. S3 D). In our earlier study, we had not tested the kinase dependence of the adhesion phenotype we observed (Wells et al., 2010). Unexpectedly, we now find that we can rescue the adhesion phenotype with exogenous expression of kinase-inactive PAK4 or exogenous expression of RhoU (Fig. 5 A). This places RhoU firmly downstream of PAK4, and we hypothesized that perhaps it was in fact RhoU that drives paxillin S272 phosphorylation in a PAK4-dependent manner. Interestingly, exogenous RhoU overexpression in a PAK4-depleted background increases the level of paxillin S272 to an amount comparable to that of control cells (Fig. 7 A), and consistent with this result, we find RhoU in a complex with paxillin (Fig. 7 B). This finding argues for an additional kinase in the PAK4–RhoU complex mediating paxillin S272 phosphorylation. In support of this hypothesis, we noted that incubation with the serine/threonine and tyrosine kinase inhibitor staurosporine dramatically reduced the level of paxillin S272 in PAK4-depleted cells overexpressing RhoU (Fig. 7 C), thus suggesting the PAK4–RhoU complex does indeed act as a scaffold to support paxillin S272 phosphorylation.

were used to pull down HA-RhoU, HA-ΔNRhoU, HA-RhoUΔC, and HA-ΔNRhoUΔC. Samples were analyzed by anti-HA immunoblotting and Coomassie staining. Representative of three independent experiments. (F) GST or GST-PAK4 (H19, 22L) beads were used to pull down GFP-Cdc42V12 or GFP-RhoU from HEK-293 cell lysates. Blot is representative of three separate experiments. Ctrl, control.

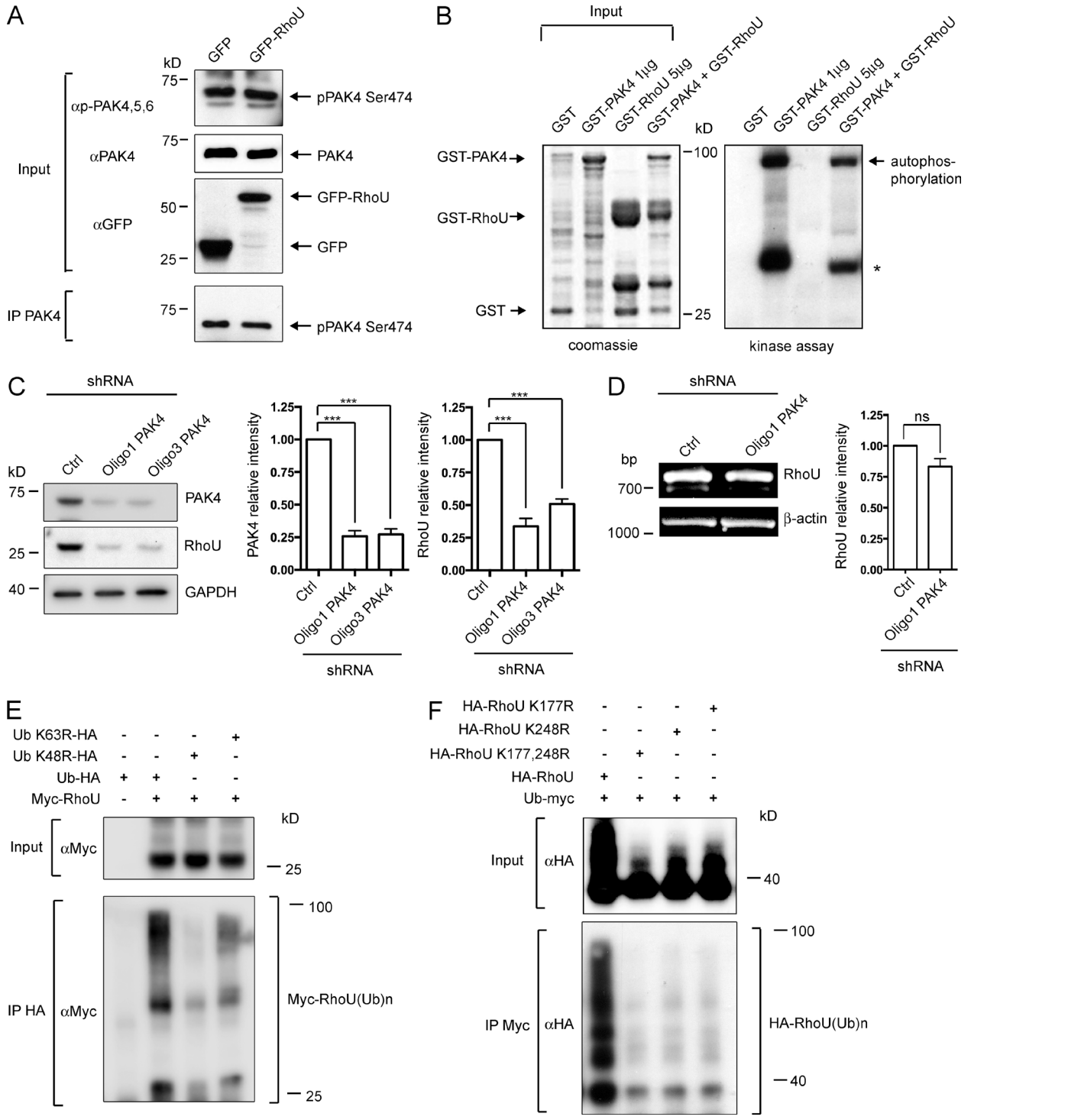

Figure 3. **RhoU undergoes K48-linked ubiquitination.** (A) Anti-PAK4 antibody was used to precipitate phospho-PAK4 (S474) from GFP or GFP-RhoU–transfected MDA-MB-231 cell lysates. (B) An in vitro kinase assay was performed using 1 μg purified GST-PAK4 and 5 μg GST-RhoU. (Left) Coomassie staining demonstrates purified protein input. (Right) Phosphorylation was detected by autoradiography. The asterisk denotes a nonspecific band always observed in PAK4 kinase assays. (C) Lysates were made from control- and PAK4 shRNA-expressing MDA-MB-231 cells and analyzed by immunoblotting with anti-PAK4 and RhoU antibodies. GAPDH was used as a loading control. Autoradiographs were quantified using ImageJ software, and the relative intensity of the PAK4 and RhoU signal was normalized to the loading control. The results shown are the means ± SEM of at least three independent experiments. ***, $P < 0.001$. (D) mRNA expression of RhoU and β-actin in control and PAK4 knockdown MDA-MB-231 cells as determined by RT-PCR. The relative intensity of the RhoU signal was normalized to the levels of β-actin. The results shown are the means ± SEM of three independent experiments. ns, not significant. (E) Anti-HA antibody coimmunoprecipitation of HA-Ub species and myc-RhoU from HEK-293 cells expressing HA-RhoU and either HA-Ub WT, HA-Ub K48R, or HA-Ub K63R. (F) Anti-Myc antibody coimmunoprecipitation of myc-Ub and HA-RhoU from HEK-293 cells expressing myc-Ub, HA-RhoU point mutants (expression plasmids with a lysine to arginine substitution at positions 177, 248, or both 177 and 248 as indicated), and GFP-PAK4. Ctrl, control.

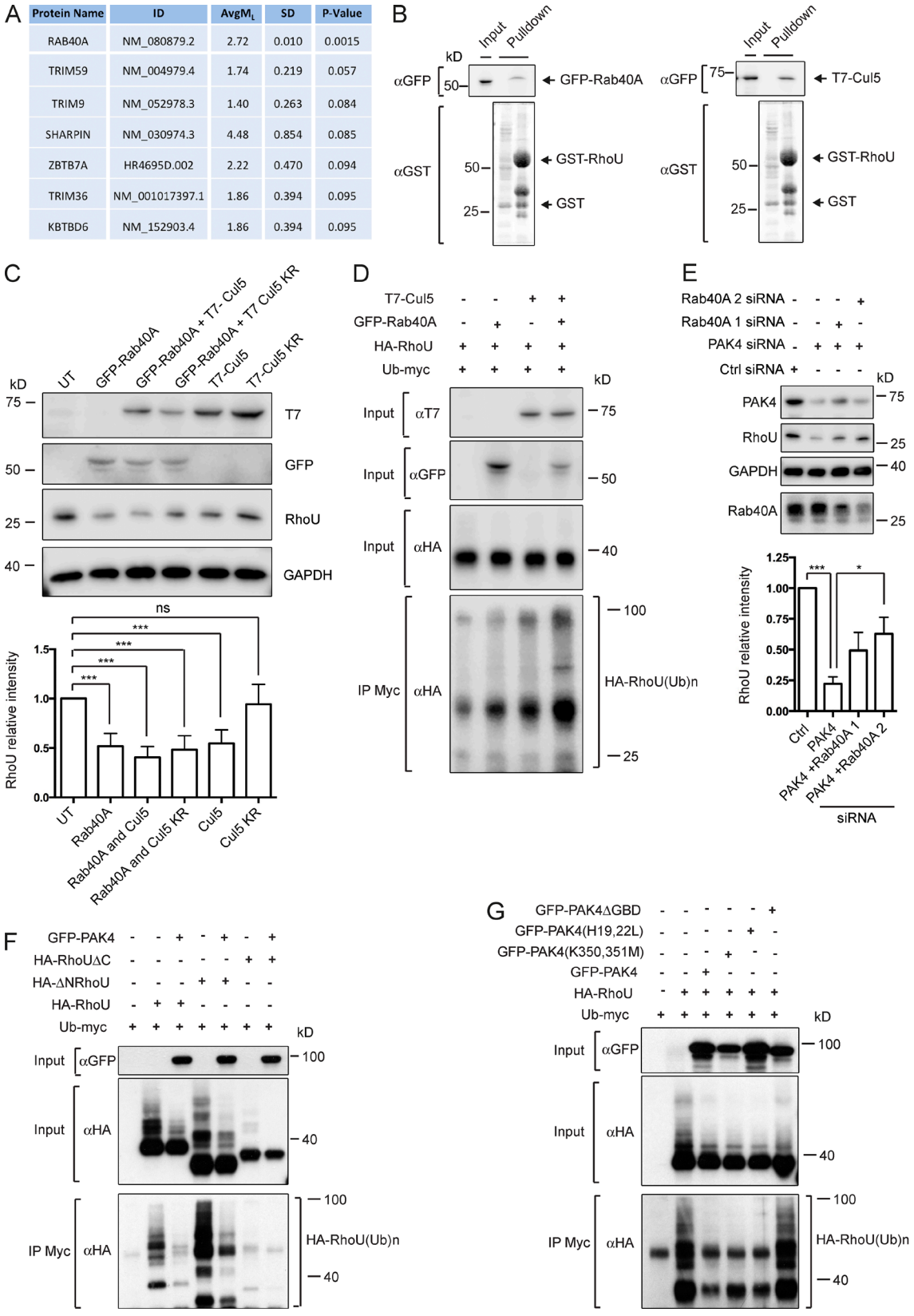

Figure 4. **RhoU interacts with the E3 Ub ligase component Rab40A and is protected from ubiquitination by PAK4.** (A) Protein microarray of RhoU–E3 ligase interactions. Column headers are as follows: ID, GenBank accession number; $AvgM_L$, duplicate-summarized, loess-normalized, log_2-transformed fluorescence intensity values obtained from the experimental array, minus those obtained from the negative control array; SD, standard deviation of the difference. P-value was calculated using a paired two-tailed *t* test for significance. $P < 0.05$ was considered to be statistically significant. (B) GST-RhoU pull-down of GFP-Rab40A and T7–Cullin 5 (Cul5). Samples were analyzed by anti-GFP and T7 immunoblotting and Coomassie staining. Representative of three independent experiments. (C) Lysates were made from HEK-293 cells expressing GFP-Rab40A and/or T7–Cullin 5 (Cul5) or T7–Cullin 5 K799R (Cul5 KR)

PAK4 and RhoU expression is correlated across breast cancer cell lines

Collectively, our data point to an important regulatory relationship between PAK4 and the level of RhoU expression whereby RhoU is targeted for ubiquitination unless interacting with PAK4. This relationship drives adhesion turnover and promotes cell migration. Together with our tissue microarray observations (Fig. 1 A), these data point to a role for PAK4 in promoting breast cancer progression. In line with this critical function of PAK4 in regulating the protein stability of RhoU, we observed a positive correlation ($R^2 = 0.712$) between PAK4 and RhoU protein levels in a panel of breast cancer cell lines (Fig. 7, D and E). Furthermore, both RhoU and PAK4 expression are elevated in metastatic MDA-MB-231 cells compared with a nontumorigenic (MCF-10A) control (Fig. 7 F), thus providing further evidence that an important physiological function of PAK4 is to stabilize cellular levels of RhoU to allow efficient cell migration.

Discussion

We found here that there is an unexpected kinase-independent role for PAK4 during cell substratum adhesion turnover. We also found that PAK4-mediated adhesion dynamics do not require kinase activity or interaction with Cdc42. Rather, we have identified a novel kinase-independent function for PAK4 in positively regulating the protein levels of RhoU. We have discovered that RhoU is preferentially K48 ubiquitinated and that this ubiquitination occurs on residues K177 and K248 of RhoU. Furthermore, we demonstrate that a Rab40A–Cullin 5 complex targets RhoU for ubiquitination in PAK4-depleted cells. We now present a novel mechanistic pathway whereby PAK4 stabilization of RhoU directly influences the level of paxillin S272 phosphorylation. Collectively, these studies place PAK4 and RhoU at the center of cell substratum adhesion dynamics during migration.

An analysis of 300 human breast cancer samples revealed that PAK4 expression was significantly associated with a high tumor grade that often leads to a poorer prognosis, the first time this has been reported in breast cancer. This result is even more significant given our finding that some important functions of PAK4 are not dependent on kinase activity, but on levels of expression.

In mesenchymal-like MDA-MB-231 cells and colony-forming MCF-7 cells, we found that reduced PAK4 expression led to an increase in cell adhesion. This phenotype was also reported by us for colony-forming DU145 cells, where we demonstrated that the increased number and size of peripheral adhesions is a direct consequence of reduced adhesion disassembly (Wells et al., 2010). In contrast, we did not find an adhesion phenotype in PAK4-depleted mesenchymal-like PC3 cells (Ahmed et al., 2008; Whale et al., 2013). These divergent phenotypes likely reflect the predominance of one PAK4 signaling nexus over another in different cell types. Indeed, the work with PC3 cells had been performed in a background of hepatocyte growth factor stimulation (Ahmed et al., 2008; Whale et al., 2013).

PAKs have been traditionally recognized to function downstream of the Rho family GTPases as effectors in a linear signaling cascade (Abo et al., 1998) where kinase activity is central to cellular outcome. However, we found no requirement for Cdc42 binding. Unexpectedly, we identified an interaction between RhoU and PAK4 that does not follow this effector convention. Although RhoU shares considerable sequence and functional similarity with the classical Rho GTPase Cdc42, it also has atypical characteristics that differentiate it. As an unconventional Rho GTPase, RhoU is believed to be constitutively active (Saras et al., 2004; Shutes et al., 2004), making its regulation different from that of the guanine nucleotide exchange factor (GEF)–mediated mechanism of Cdc42 (Shutes et al., 2004). We reveal that RhoU, similar to other Rho GTPases (Nethe and Hordijk, 2010), is ubiquitinated, thus providing a novel mechanism through which RhoU signaling output can be controlled. In addition, we show that RhoU is primarily modified by K48-linked polyubiquitin chains, likely acting as a proteolytic signal to target RhoU for proteasome-mediated degradation. However, we cannot rule out K63-linked ubiquitination; this form of post-translational modification is thought to regulate the subcellular localization of the target protein (Wang et al., 2012), and K63 linkage could influence RhoU accumulation into endosomes as a means of limiting RhoU-driven signaling.

By screening a human proteome microarray, we were able to identify an interaction between RhoU and Rab40A, a small GTP-binding protein. Rab40A contains a substrate recognition motif known as a SOCS (suppressor of cytokine signaling) box. This motif in other proteins has been shown to provide substrate specificity, and through direct binding to the substrate, it bridges the target protein to Elongin and Cullin proteins, which together constitute a multisubunit ECS complex with Ub ligase activity (Kile et al., 2002). In *Xenopus*, XRab40 (the homologue of human Rab40A) is one component of an E3 Ub ligase, along with ElonginB/C and Cullin 5. As such, the XRab40-containing ECS complex ubiquitinates the GTPase Rap2 that in turn regulates its localization and influence over downstream effectors in the noncanonical Wnt signaling pathway (Lee et al., 2007). It has already been established that Wnt signaling can regulate expression levels of RhoU (Schiavone et al., 2009; Dickover et al., 2014), and notably, we also identified Wnt6 (Kirikoshi et al., 2001) as a putative interacting partner of RhoU (Table S1). Hence, we predicted that RhoU could be a substrate for ubiquitination by a Rab40A-containing complex in humans, and in validation, we showed that overexpression of Rab40A can reduce endogenous levels of RhoU through its enhanced

and immunoblotted with anti-GFP and RhoU antibodies. GAPDH was used as a loading control. UT, untransfected. Autoradiographs were quantified using ImageJ software, and the relative intensity of the RhoU signal was normalized to the loading control. The results shown are the means ± SEM of at least three independent experiments. ***, P < 0.001. ns, not significant. (D) Coimmunoprecipitation of myc-Ub and HA-RhoU from HEK-293 cells expressing myc-Ub, HA-RhoU, and either GFP-Rab40A, T7–Cullin 5 (Cul5), or GFP-Rab40A and T7–Cullin 5. (E) Lysates from MDA-MB-231 cells where PAK4 had been silenced or PAK4 had been silenced in combination with Rab40A after 48 h and immunoblotted with anti-PAK4, RhoU, and Rab40A antibodies. GAP DH was used as a loading control. Autoradiographs were quantified using ImageJ software, and the relative intensity of the RhoU signal was normalized to the loading control. The results shown are the means ± SEM of at least three independent experiments. *, P < 0.05; ***, P < 0.001. (F) Anti-Myc antibody coimmunoprecipitation of myc-Ub and HA-RhoU from HEK-293 cells expressing myc-Ub, HA-RhoU domain mutants, and GFP-PAK4. (G) Anti-Myc antibody coimmunoprecipitation of myc-Ub and HA-RhoU from HEK-293 cells expressing myc-Ub, HA-RhoU, and GFP-tagged PAK4 mutants. Ctrl, control.

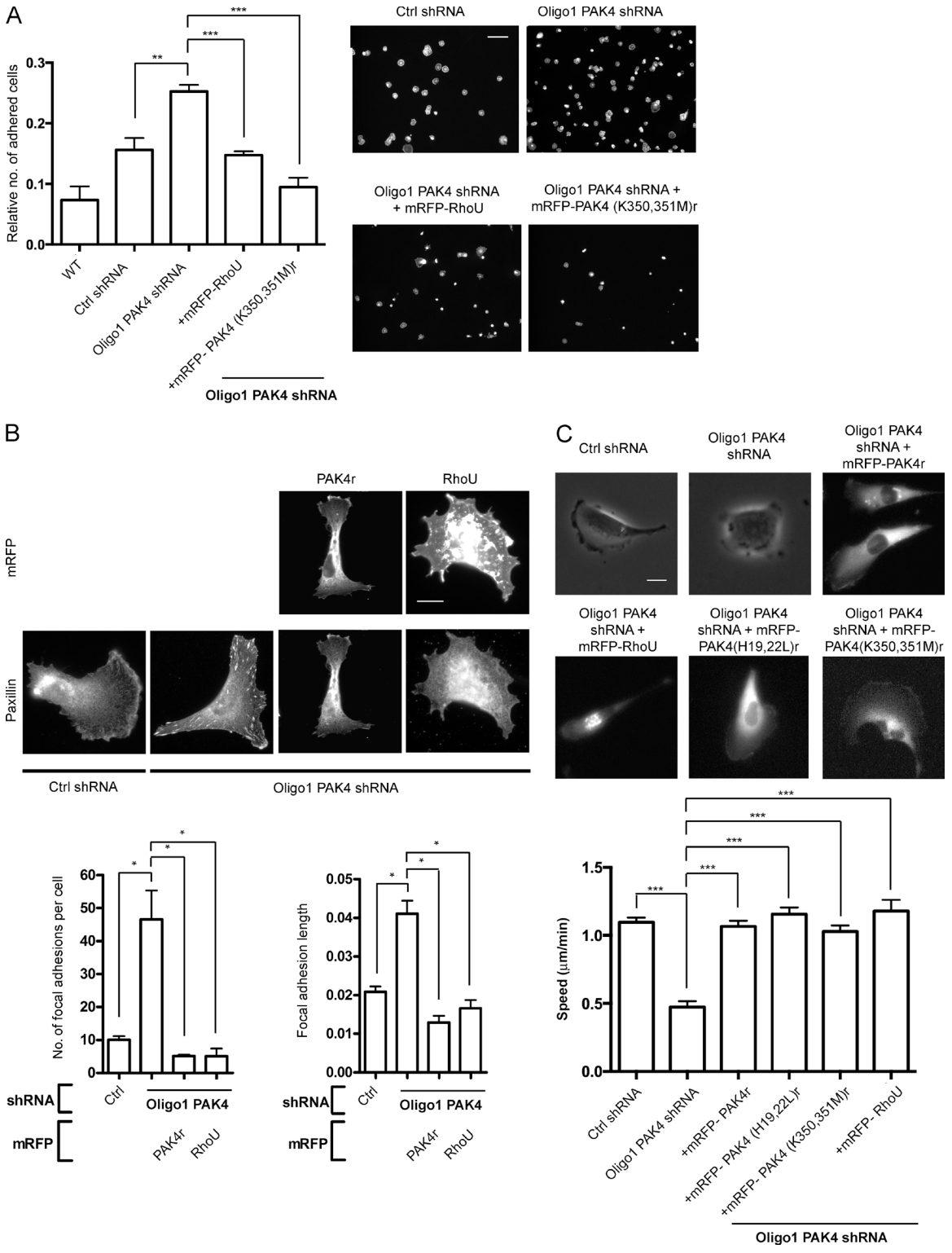

Figure 5. **RhoU functions downstream of PAK4 in MDA-MB-231 cell adhesion and migration.** (A, left) Adhesion assay of Oligo1 PAK4-depleted MDA-MB-231 cells expressing GFP-RhoU or shRNA-resistant mRFP-PAK4 (K350, 351M) plated onto 10 µg/ml fibronectin for 60 min. The relative number of adhered cells is absorbance at 560 nm. **, $P < 0.01$; ***, $P < 0.001$. (Right) F-actin staining of these same cell conditions plated onto 10 µg/ml fibronectin and fixed after 60 min. Bar, 100 µm. (B) Paxillin labeling of control and Oligo1 PAK4-depleted MDA-MB-231 cells expressing either shRNA-resistant mRFP-PAK4 or mRFP-RhoU. Bar, 20 µm. The mean number of focal adhesions and the mean length of focal adhesions for Oligo1 PAK4 shRNA-expressing MDA-MB-231 cells also expressing mRFP-RhoU or shRNA-resistant mRFP-PAK4 were measured using ImageJ software. $n > 60$ cells per condition over three independent experiments. *, $P < 0.05$. (C) Control and Oligo1 PAK4-depleted MDA-MB-231 cells expressing shRNA-resistant mRFP-PAK4, -PAK4 (H19, 22L), -PAK4 (K350, 351M), or mRFP-RhoU plated onto 10 µg/ml fibronectin were filmed for 18 h with time-lapse video microscopy. Mean migration speed ± SEM was calculated by tracking 60 individual cells per population (*n*) over three separate experiments. ***, $P < 0.001$. Image stills from the videos depicting typical cell morphologies. Bar, 20 µm. Ctrl, control.

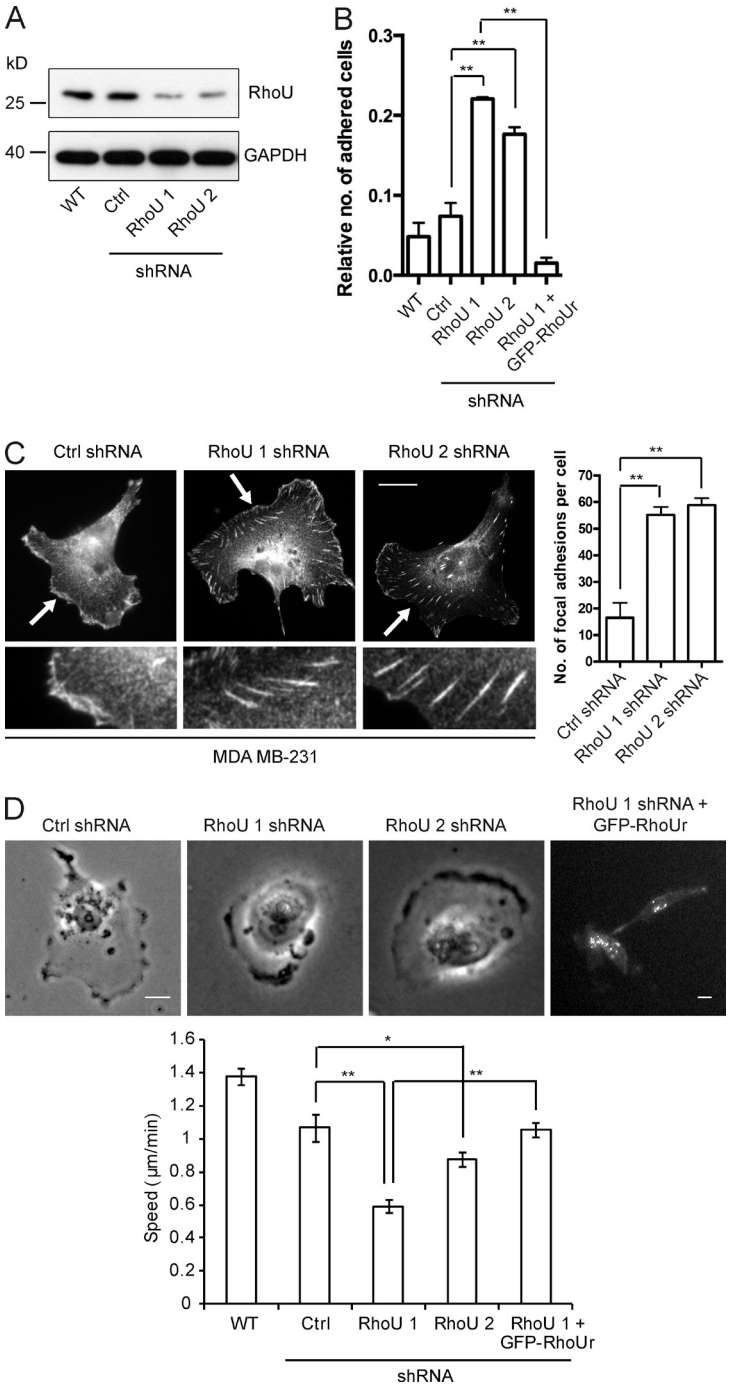

Figure 6. **RhoU controls MDA-MB-231 cell adhesion and motility.** (A) WT MDA-MB-231 cells were transiently transfected with control or RhoU (1 and 2) shRNA, and protein levels were determined after 48 h by immunoblotting. (B) Adhesion assay of WT, control, and RhoU shRNA-expressing MDA-MB-231 cells plated onto 10 µg/ml fibronectin for 60 min. The relative number of adhered cells is absorbance at 560 nm. Error bars represent mean ± SEM. **, $P < 0.01$. (C) Paxillin labeling of MDA-MB-231 cells transiently expressing control or RhoU shRNA. The arrows highlight magnified insets. Bar, 20 µm. The mean number of focal adhesions per cell for all cell populations were measured using ImageJ software. $n > 60$ cells per condition over three independent experiments. **, $P < 0.01$. (D) Control and RhoU shRNA-expressing MDA-MB-231 cells plated onto 10 µg/ml fibronectin were filmed for 18 h with time-lapse video microscopy. Mean migration speed ± SEM was calculated by tracking 60 individual cells per population (*n*) over three separate experiments. *, $P < 0.05$; **, $P < 0.01$. Image stills from the videos depict typical cell morphologies. Bar, 20 µm. Ctrl, control.

ubiquitination. Interestingly, we were also able to demonstrate that overexpressed Cullin 5 leads to a decreased level of RhoU, and together with Rab40A, overexpression resulted in an additive effect on RhoU degradation and ubiquitination. Our data, although identifying Rab40A as a key E3 ligase component for RhoU ubiquitination, also highlighted that other potential E3 ligases (such as Sharpin) may either compensate for the function of Rab40A or be acting autonomously on RhoU, a finding that would seemingly fit with RhoU being ubiquitinated on more than one site and undergoing two types of lysine linkage additions. It will be important in the future to investigate the full impact of Sharpin function on RhoU. It should be noted that because of the stringent binding conditions used to perform the microarray, only tight regulatory interactions were revealed, likely explaining why PAK4 and PAK1 were not identified as highly significant hits.

Our data clearly demonstrate that PAK4 is able to protect RhoU from ubiquitination, independent of kinase function. PAK4 protection is delivered through the GBD of PAK4, a novel function for this domain, and to our knowledge, this is the first example of positive modulation of protein levels by PAK4. Therefore, we present PAK4 as a novel regulator of RhoU function rather than the accepted term "effector." Indeed, we have found that PAK4 and RhoU expression is correlated in a panel of breast cancer cell lines, suggesting that the relationship between PAK4 and RhoU expression is not confined to the cell types studied here. In agreement with the model that up-regulation of PAK4 and RhoU can promote migratory phenotypes in

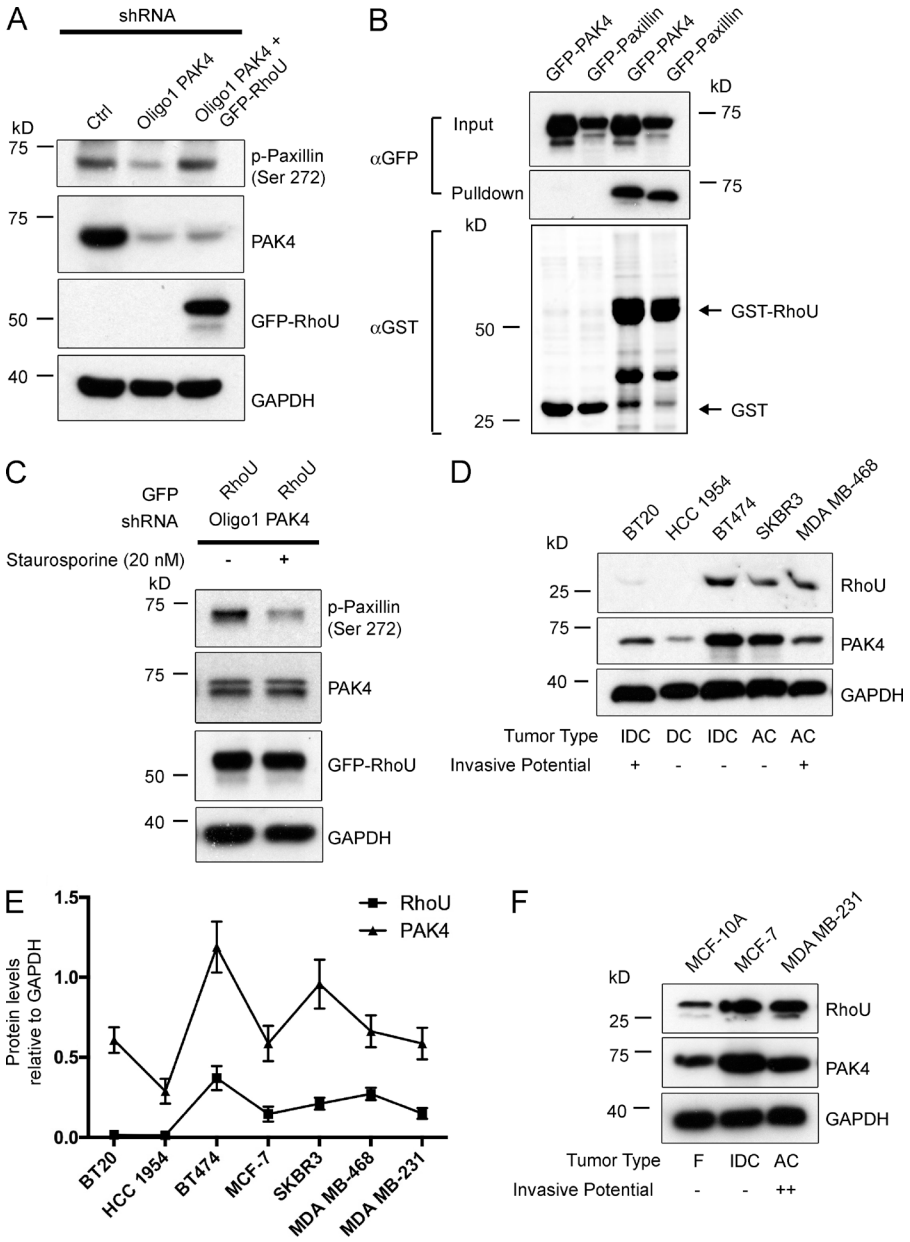

Figure 7. **RhoU can influence the serine phosphorylation of paxillin.** (A) Blots showing the levels of paxillin (S272) in control and PAK4 shRNA MDA-MB-231 cells overexpressing GFP-RhoU plated onto 10 µg/ml fibronectin. (B) GST-RhoU beads were used to pull down overexpressed GFP-PAK4 and GFP-paxillin from MDA-MB-231 cell lysates. Representative of three separate experiments. (C) Blots showing the levels of paxillin (S272) in PAK4 shRNA MDA-MB-231 cells overexpressing GFP-RhoU in the absence (DMSO control) or presence of 20-nM staurosporine. All cells were plated onto 10 µg/ml fibronectin. (D) Immunoblot analysis of RhoU and PAK4 protein expression in breast tumorigenic cell lines. (E) Densitometry analyses of RhoU and PAK4 levels relative to levels of the GAPDH loading control in breast tumorigenic cell lines. Values are means ± SEM from at least three experiments. Squared correlation value between PAK4 and RhoU (R^2) equals 0.712. (F) Immunoblot analysis of RhoU and PAK4 protein expression in a mammary epithelial cell line (MCF-10A) compared with breast cancer cells MCF-7 and MDA-MB-231. For D and F, labels are as follows: IDC, invasive ductal carcinoma; DC, ductal carcinoma; AC, adenocarcinoma; F, fibrocystic disease, nontransformed, immortal cell line. Invasive potential is defined as not invasive (–), invasive (+), and highly invasive (++; Tong et al., 1999; Neve et al., 2006). Ctrl, control.

breast carcinoma are the observations that Rab40A (Oncomine Research Edition; Neve and Bild datasets accessed May 2015) and Cullin 5 (Fay et al., 2003) genes are frequently underexpressed in breast cancer cell lines and tissues.

Interestingly, Rac1 Ub conjugates localize preferentially to endosomal structures, whereas a mutant of Rac1 that cannot be ubiquitinated displays increased accumulation at the plasma membrane (Nethe et al., 2010). In agreement with this, we have noted an increase in vesicular RhoU upon expression of the ΔN mutant that is heavily ubiquitinated, contrasting with the expression of the ΔC mutant that is not present in vesicles (unpublished data). Consistent with the notion that ubiquitination of RhoU could drive its subsequent internalization into EEA1-positive endosomes is the functioning of Rab GTPases in vesicle trafficking and, more specifically, of Rab40 in recycling endosomes (Jean and Kiger, 2012). Moreover, this type of signaling pathway has parallels with that of H-Ras, which is ubiquitinated by Rab5 GEF Rabex-5, resulting in its sequestration into early endosomes and most likely preventing its interaction with downstream effectors (de la Vega et al., 2011). It is also an attractive possibility to speculate that the interaction between RhoU and PAK4, besides providing protection from ubiquitination, could offer a reciprocal advantage in localization. Interactions between Cdc42 and PAK4 have been shown to target the kinase to specific cellular compartments, such as the Golgi apparatus and cell–cell adherens junctions (Abo et al., 1998; Wallace et al., 2010). Therefore, in a similar manner, it may be that RhoU could spatially restrict PAK4 at focal adhesions.

RhoU has been implicated in focal adhesion dynamics previously, but its exact role has been controversial. RhoU accumulates in osteoclast podosomes as well as the focal adhesions of HeLa and NIH 3T3 cells (Chuang et al., 2007; Ory et al., 2007) and is linked to adhesion disassembly. In contrast, in T-ALL cell lines, RhoU promotes adhesion (Bhavsar et al., 2013). However, we find that a loss of RhoU expression in MDA-MB-231 cells de-

livers increased adhesion. Moreover, the depletion of RhoU drives the same phenotype as the loss of PAK4 in these cells, again suggesting that these two proteins coordinate to regulate adhesion turnover.

We have previously reported that PAK4 can phosphorylate paxillin at S272 in vitro and that S272 phosphorylation of paxillin is a driver of adhesion disassembly (Wells et al., 2010). Consistent with our earlier work, paxillin S272 phosphorylation was reduced upon depletion of PAK4 in MDA-MB-231 cells. Furthermore, we found no evidence for PAK1 regulation of paxillin S272 phosphorylation. Recently, an alternative pathway to focal adhesion disassembly was reported in endothelial cells that requires RhoJ and the GIT–PIX complex (Wilson et al., 2014) with the implication that PAK1 is required. However, PAK4 does not interact with RhoJ, a cycling Rho GTPase whose regulation is likely to be via GEF activity (Vignal et al., 2000). PAK1 protein levels are normal in our PAK4-depleted cells, and therefore PAK1 is unable to compensate for a loss of PAK4 with respect to paxillin phosphorylation. Indeed, PAK1 does not phosphorylate paxillin at S272 in vitro (Dong et al., 2009), and in our hands, the depletion of PAK1 does not alter focal adhesion dynamics in breast cancer cells. We thus conclude that PAK4 is the predominant PAK species regulating paxillin-mediated focal adhesion turnover in breast cancer cells. Moreover, we now believe that although PAK4 can phosphorylate paxillin in vitro, in cellulo PAK4 delivers paxillin phosphorylation in a kinase-independent manner via stabilization of RhoU (Fig. 8).

This unexpected conclusion is derived from our data revealing that overexpression of RhoU could elevate the level of paxillin S272 phosphorylation in PAK4-depleted cells. Overexpression of RhoU could allow residual PAK4 to be targeted to paxillin, but we have extremely low levels of PAK4 expression in our knockdown cells, and our data firmly argue for a kinase-independent pathway, given that kinase-dead PAK4 can rescue the adhesion phenotype. Thus, it is more likely that we have identified an alternative signaling pathway to paxillin S272 phosphorylation. Indeed, we were able to show that RhoU exerts its actions through a staurosporine-sensitive mechanism. Staurosporine inhibits a range of kinases such as PKC, PKA, PKG, and myosin light chain kinase (Omura et al., 1995), and as such, we can only speculate on the precise nature of the protein kinase modulated by RhoU. Of these candidates, myosin light chain kinase is an attractive possibility given that RhoU depletion can decrease myosin regulatory light chain phosphorylation (Chuang et al., 2007). Another hypothesis is that RhoU, via PKA, could produce a positive reinforcing feedback loop by virtue of the capacity of PKA itself to phosphorylate PAK4 (Park et al., 2013). Thus, the relationship between PAK4, RhoU, and PKA warrants further study.

In conclusion, we present a new view on the role of PAK4 in cell adhesions where a major function of PAK4 is to stabilize RhoU, which in turn leads to focal adhesion disassembly via phosphorylation of paxillin. We further propose that PAK4 expression is a component of breast cancer progression, thus supporting the notion that PAK4 is an attractive candidate drug target. However, to date, all PAK4-specific inhibitors developed have been competitive ATP inhibitors (Murray et al., 2010; Zhang et al., 2012). In light of our findings, we suggest that efforts should also be made to develop allosteric inhibitors that could ultimately provide significant target selectivity.

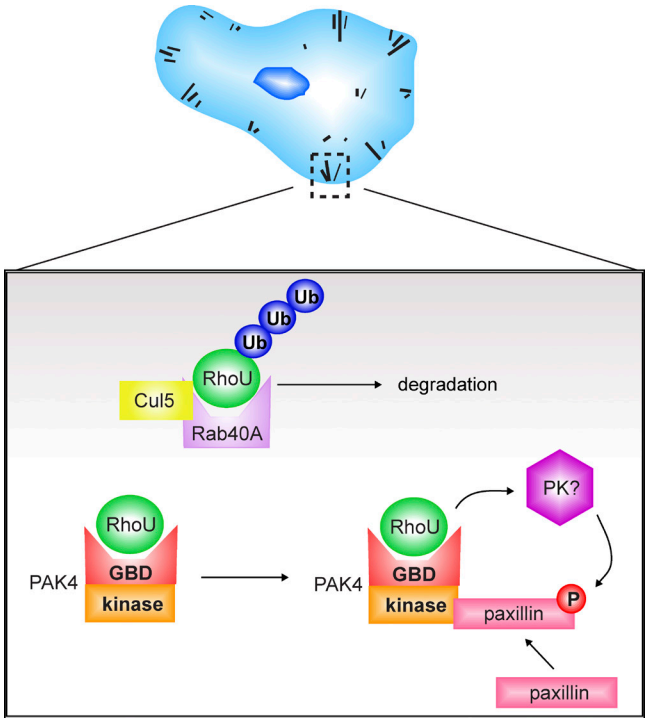

Figure 8. **PAK4 drives kinase-independent stabilization of RhoU to regulate cell adhesion and motility.** Schematic illustrating how PAK4 and RhoU converge on paxillin phosphorylation at S272. PAK4 regulates the stability of RhoU through protection from ubiquitination by a Rab40A–Cullin 5 complex and scaffolds paxillin, allowing RhoU to drive modulation of paxillin S272 phosphorylation. Ultimately, this signaling contributes to focal adhesion disassembly and, consequently, efficient cell migration.

Materials and methods

Antibodies and reagents

Unless indicated, primary antibodies were used at a dilution of 1:1,000 for Western blotting. Anti-GAPDH was purchased from EMD Millipore and used at a dilution of 1:20,000. Rabbit anti-PAK1, rabbit anti–phospho-PAK4 (S474)/PAK5 (S602)/PAK6 (S560), and rabbit anti-PAK4, which also recognizes PAK6 (Ahmed et al., 2008), were purchased from Cell Signaling Technology. Rabbit polyclonal PAK4-specific antibody (raised against PAK4 peptide sequence CRRAGPEKRPKSS REG) has been described elsewhere (Wells et al., 2010). Rabbit anti-RhoU (Wrch1) and rabbit anti-Rab40A were obtained from Abcam and used at a dilution of 1:500. Mouse anti-GFP was obtained from Roche and mouse anti-T7 from EMD Millipore. Rabbit anti-HA (Y-11) and mouse c-Myc (9E10) were purchased from Santa Cruz Biotechnology, Inc. Mouse antipaxillin were obtained from BD, rabbit anti-phosphopaxillin S273(272) from Invitrogen, and mouse antivinculin from Sigma-Aldrich. HRP-conjugated secondary antibodies were purchased from Dako and diluted 1:2,000. Staurosporine was purchased from Cell Signaling Technology and dissolved in DMSO.

DNA constructs

Vectors encoding myc-Ub, GFP-Cdc42V12, and GFP-RhoU were gifts from R. Kopito (Stanford University, Stanford, CA), M. Parsons (King's College London, London, England, UK), and P. Aspenstrom (Karolinska Institute, Stockholm, Sweden), respectively. Vectors encoding GFP-tagged RhoU effector point mutants (T81S, F83A, F86C, and 3M) were a gift from A. Blangy (Centre National de la Recherche Scientifique, Montpellier, France). HA-Ub, HA-Ub K48R, and HA-Ub

K63R were all gifts from K.L. Lim (National Neuroscience Institute, Singapore). T7–Cullin 5 and T7–Cullin 5 (K799R) were gifts from J.A. Cooper (Fred Hutchinson Cancer Research Center, Seattle, WA), and GFP-Rab40A and GFP-Sharpin were gifts from J. Ramalho (Centro de Estudos de Doencas Cronicas, Lisbon, Portugal) and J. Ivaska (Turku Centre for Biotechnology, Turku, Finland), respectively. cDNA of PAK4, PAK4r (containing silent shRNA refractory mutations), GBD domain (amino acids 1–30), ΔGBD domain (amino acids 30–591), kinase domain (encoding amino acids 323–591), Δkinase domain (amino acids 1–322), PAK4 (H19, 22L), PAK4 (H19, 22L)r, and PAK4 (K350, 351M)r was previously cloned into pDONR207 using BP recombination (Gateway; Thermo Fisher Scientific) to generate entry vectors (Wells et al., 2010; Whale et al., 2013). PAK4 derivatives were then transferred into either mammalian mRFP or bacterial GST expression destination vectors using LR recombination (Gateway). PAK1, RhoU, ΔNRhoU (encoding amino acids 45–258), RhoUΔC (amino acids 1–223), and ΔNRhoUΔC (amino acids 45–223) cDNA was cloned into pDONR207 using BP recombination to generate pENTR-RhoU, -ΔNRhoU, -RhoUΔC, and -ΔNRhoUΔC, respectively. The *RhoU* derivatives were then transferred into either mammalian 3xHA or bacterial GST and HIS expression vectors using LR recombination. Point mutations were introduced into pENTR-RhoU using primers designed with the mutagenic primer design program (QuikChange; Agilent Technologies). The mutagenesis kit was used according to manufacturer's instructions to generate a pENTR-RhoUr (containing silent shRNA refractory mutations) and multiple pENTR-RhoU K-to-R mutants. Clones were screened by sequencing and aligned to the WT sequence to confirm mutagenesis. The sequence-verified mutant was then transferred into mammalian mRFP and EGFP expression destination vectors using linker region recombination. All constructs were verified by sequencing.

Cell culture and transfection

MDA-MB-231 breast adenocarcinoma cells and all other breast cancer cell lines were obtained from the European Tissue Culture Collection and grown in complete DMEM (Sigma-Aldrich) supplemented with 10% FCS (Sigma-Aldrich) and 100 U/ml penicillin-streptomycin. MDA-MB-231 cells were transiently transfected using Lipofectamine 2000 transfection reagent (Invitrogen) according to the manufacturer's protocol. HEK-293 cells (European Tissue Culture Collection) were grown in complete DMEM, supplemented with 10% FCS and 100 U/ml penicillin-streptomycin, and transfected by calcium-phosphate transfection according to the manufacturer's protocol. For inhibitor experiments, staurosporine was incubated with cells in a serum-starved medium at a final concentration of 20 nM for 3 h before lysis.

shRNA and siRNA transfection

To generate stable control and PAK4 knockdown MDA-MB-231 cell lines, cells were transfected with control or PAK4-specific pGIPz lentiviral bicistronic vectors using Lipofectamine 2000 according to the manufacturer's protocol. Open Biosystems Oligo IDs were as follows: nonsilencing control RHS4346 (sequence 5′-ATCTCGCT TGGGCGAGAGTAAG-3′), Oligo1 V2LHS_197812 (sequence 5′-CTGGACAACTTCATCAAGA-3′), and Oligo3 V3LHS_646396 (sequence 5′-CGATCATGAATGTCCGAAG-3′). Stable cell lines were puromycin selected (700 ng/ml) before cell sorting to isolate TurboGFP-expressing cells (polyclonal cells) and maintained in a medium supplemented with 700 ng/ml puromycin. Knockdown of RhoU was achieved by transient transfection of pLKO.1 vectors containing RhoU shRNA inserts (RhoU1 sequence 5′-CGGACAGGATGAATTTGA CAA-3′ and RhoU2 sequence 5′-CTACATCGAGTGTTCAGCCTT-3′), a gift from A. Ridley (King's College London, London, England, UK), using Lipofectamine 2000. Transient knockdown of PAK4 in MCF-7 cells was achieved using human PAK4 siRNA oligonucleotide 2 (S102660315; sequence 5′-CGAGAATGTGGTGGAGATGTA-3′; QIAGEN) and oligonucleotide 5 (D-003615-05; sequence 5′-GGG TGAAGCTGTCAGACTT-3′; GE Healthcare). Transient knockdown of PAK1 and PAK2 in MDA-MB-231 cells was achieved using SMA RTpool ON-TARGETplus human PAK1 siRNA (L-003521-00-0005; sequences 5′-GGAGAAAUUACGAAGCAUA-3′, 5′-UCAAAUAA CGGCCUAGACA-3′, 5′-ACCCAAACAUUGUGAAUUA-3′, and 5′-CAUCAAAUAUCACUAAGUC-3′; GE Healthcare) and SMA RTpool ON-TARGETplus human PAK2 siRNA (L-003597-00-0005; sequences 5′-GAAACUGGCCAAACCGUUA-3′, 5′-GAGCAGAG CAAACGCAGUA-3′, 5′-ACAGUGGGCUCGAUUACUA-3′, and 5′-GAACUGAUCAUUAACGAGA-3′; GE Healthcare). Transient knockdown of Rab40A was attained by using individual human siGENOME Rab40A siRNA oligonucleotides 1 and 2 (D-008924-01 and D-008924-05; sequences 5′-GCAAACCGCUGGUCUUUCG-3′ and 5′-GGG UAUGGAUCGAUGGAUU-3′, respectively; GE Healthcare). Control RNA oligonucleotides were purchased from QIAGEN (1022076; sequence 5′-AATTCTCCGAACGTGTCACGT-3′). Control and *PAK4*-, *PAK1*-, *PAK2*-, and *Rab40A*-specific oligonucleotides were added to cells using a HiPerFect Transfection Reagent (QIAGEN) according to the manufacturer's instructions to a final concentration of 30 nM. Efficiency of knockdown was assessed by Western blotting after 48 h.

Immunofluorescence and image analysis

Cells were seeded onto human fibronectin (10 µg/ml; Sigma-Aldrich)-coated coverslips. After transfection or incubation overnight, cells were fixed in 4% paraformaldehyde in PBS for 20 min at RT and subsequently permeabilized with 0.2% Triton X-100 in PBS for 5 min. For F-actin staining, cells were incubated with either TRITC- or Alexa Fluor 488–conjugated phalloidin (Invitrogen) and diluted in PBS for 1 h at RT. After this incubation, cells were washed three times in PBS. For detection of paxillin, primary antibodies were diluted in PBS with 3% BSA (Thermo Fisher Scientific) and incubated for 2 h at RT. After labeling with the primary antibodies, cells were washed three times with PBS before incubation with either Alexa Fluor 568– or 488–conjugated secondary antibodies (Invitrogen) and phalloidin. Cells were then imaged using either a microscope (IX71; Olympus) with a 40× oil-immersion objective (UPlanFLN) with a numerical aperture of 1.3 and Image-Pro Plus software (Media Cybernetics) or a confocal laser-scanning microscope (LSM510; Carl Zeiss) with a Plan Fluorite 100× oil objective with a numerical aperture of 1.45 and the accompanying LSM510 software. Focal adhesion number and length were quantified using ImageJ software (National Institutes of Health).

Time-lapse microscopy

Cells were plated onto fibronectin-coated 6-well plates, to which 25-mM Hepes was added. Immediately before filming, MCF-7 cells were treated with 100 ng/ml EGF to induce motility (Garcia et al., 2006). Each plate was placed on the automated heated stage of an microscope (IX71) set at 37°C and imaged with a 10× objective lens (UPlanFLN) with a numerical aperture of 0.3. Images were collected using a charge-coupled device camera (Retiga-SRV; QImaging), taking a frame every 5 min for 18 h from each of the wells using Image-Pro Plus software. Subsequently, all of the acquired time-lapse sequences were displayed as a video, and cells were tracked for the whole of the time-lapse sequence using motion analysis software (Andor Technology). This resulted in the generation of a sequence of position coordinates relating to each cell in each frame. At least 60 cells were tracked over three separate films for each experimental condition. Mathematical analysis was then performed using Mathematica 6.0 notebooks

(Wolfram) developed in-house by G. Dunn and G.E. Jones (King's College London, London, England, UK). Statistical significance was accepted for $P \leq 0.05$.

Adhesion assay

Cells were seeded at 5×10^4 on 24-well plates that were precoated with 10 µg/ml fibronectin (Sigma-Aldrich). After 60 min at 37°C, the cells were washed twice with PBS, incubated in 500 µg/ml methylthiazoletetrazolium (Sigma-Aldrich), and diluted in complete DMEM for 3 h to detect viable cells that were still adhered to the substrate. The converted dye was then solubilized for 10 min using DMSO. Finally, the absorbance at 540 nm was measured using an alpha fusion plate reader (PerkinElmer).

Immunohistochemical staining

In brief, formalin-fixed, paraffin-embedded human breast cancer tissue samples were stained with an in-house PAK4-specific antibody (Wells et al., 2010) using the BondMax system (Leica).

RT-PCR

Total RNA was isolated from WT, control, and PAK4 knockdown MDA-MB-231 cells using the RNeasy kit (QIAGEN) according to the manufacturer's protocol. Reverse transcription was performed with the High Capacity RNA-to-cDNA kit (Applied Biosystems) according to the manufacturer's instructions. The cDNA obtained from the reverse transcription reaction was then used in a PCR with REDTaq ReadyMix PCR Reaction Mix with $MgCl_2$ (Sigma-Aldrich). RT-PCR products were resolved by electrophoresis in 1.5% ethidium bromide–stained agarose gels.

Immunoprecipitation

Cells were lysed for 10 min in a lysis buffer (0.5% NP-40, 30-mM sodium pyrophosphate, 50-mM Tris-HCl, pH 7.6, 150-mM NaCl, 0.1-mM EDTA, 50-mM NaF, 1-mM Na_3VO_4, 1-mM PMSF, 10 µg/ml leupeptin, and 1 µg/ml aprotinin) and clarified by centrifugation at 16,200 *g* for 10 min. Cell lysates were then incubated with primary rabbit anti-PAK4 antibody or an isotype control antibody (rabbit anti–VSV-G; Bethyl Laboratories, Inc.) overnight at 4°C followed by 1-h incubation with protein A–Sepharose beads (GE Healthcare). The immune complexes were washed three times with a lysis buffer and resuspended in 2× SDS loading buffer. Proteins were resolved by SDS-PAGE as previously described (Wells et al., 2002) and immunoblotted with the relevant antibodies.

GST-tagged protein purification and pull-down assays

GST proteins were purified from BL21-A1 cells (Invitrogen). In brief, bacterial cells were transformed with pDEST15-GST-PAK4, -GBD domain, -ΔGBD domain, -kinase domain, -Δkinase domain, -(H19, 22L), or GST-RhoU expression vectors and cultured in a lysogeny broth supplemented with 100 µg/ml ampicillin until OD_{600} 0.4–0.6. Recombinant protein synthesis was induced overnight at 20°C with 0.2% L-arabinose. Bacterial pellets were lysed in PBS containing complete mini-protease inhibitor tablet (Roche) followed by sonication and centrifugation at 15,000 *g* for 10 min at 4°C to remove cell debris. The supernatant was then incubated with prewashed glutathione Sepharose 4B beads (GE Healthcare) for 2 h at 4°C, and the GST fusion protein–coupled beads were collected by centrifugation, washed three times, and stored in 50% glycerol, 20-mM Tris-HCl, pH 7.6, 100-mM NaCl, and 1-mM DTT. Transfected HEK-293 cells were lysed in 0.5% NP-40, 30-mM sodium pyrophosphate, 50-mM Tris-HCl, pH 7.6, 150-mM NaCl, 0.1-mM EDTA, 50-mM NaF, 1-mM Na_3VO_4, 1-mM PMSF, 10 µg/ml leupeptin, and 1 µg/ml aprotinin. Lysates were then precleared by incubation with glutathione Sepharose 4B beads for 1 h at 4°C. These precleared lysates were incubated with the GST fusion protein beads for 2 h at 4°C, collected by centrifugation, washed three times with a lysis buffer, and resuspended in a 2× SDS loading buffer.

Kinase assay

Bound GST-RhoU and -PAK4 proteins to be used in kinase assays were eluted from glutathione Sepharose beads and purified as follows. Beads were rotated for 30 min at 4°C in an elution buffer (100-mM Tris, pH 8, 150-mM NaCl, 5-mM reduced L-glutathione [Sigma-Aldrich], and 1-mM DTT) before being spun down at 500 *g* for 1 min. The eluate was then dialysed overnight at 4°C in a dialysis buffer (100-mM Tris, pH 8, and 150-mM NaCl) using dialysis tubing (Visking; VWR), after which purified GST proteins were incubated in a kinase buffer (50-mM Tris-HCl, pH 7.5, 10-mM $MgCl_2$, and 1-mM DTT) containing 30-µM ATP and 3 µCi γ-[^{32}P]ATP together with histone H1 (Roche) for 30 min at 30°C. The reaction was stopped by adding an SDS loading buffer.

HIS-tagged protein purification

HIS-RhoU was purified from BL21-A1 cells (Invitrogen). In brief, bacterial cells were transformed with the pDEST15-HIS-RhoU expression vector and cultured in an LB broth supplemented with 100 µg/ml ampicillin until OD_{600} 0.4–0.6. Recombinant protein synthesis was induced overnight at 20°C with 0.2% L-arabinose. Bacterial pellets were lysed in PBS containing complete mini-protease inhibitor tablets followed by sonication and centrifugation at 15,000 *g* for 10 min at 4°C to remove cell debris. The supernatant was then incubated with Ni^{2+} nitrilotriacetate agarose beads (QIAGEN) for 2 h at 4°C, and the HIS fusion protein–coupled beads were collected by centrifugation and washed extensively. For use in the subsequent Ub protein microarray, HIS-tagged RhoU was eluted from the agarose beads by incubation of the resin in 250-mM imidazole, pH 7, for 10 min with rotation and then centrifuged at 500 *g* for 5 min. The elution step was repeated once more, and the purified protein fractions were pooled. Purified protein was then dialysed overnight at 4°C in PBS using dialysis tubing (Visking).

Protein microarray

An E3 ligase identification service (LifeSensors) was used to identify the E3 ligase involved in the ubiquitination of RhoU. CDI-Labs HuProt V2.0 arrays with ∼20,000 human proteins were exposed to recombinant HIS-tagged RhoU or a buffer alone. Arrays were blocked for 1 h at RT in PBS containing 0.05% Tween 20, 20-mM reduced glutathione, 1-mM DTT, 5% BSA, and 25% glycerol. One array was treated with RhoU (100 nM) and a second, control array was treated with a buffer for 1 h at RT. Arrays were then washed three times in PBS with 0.01% Tween 20 (PBS-T) to remove soluble components followed by incubation with rabbit anti-RhoU antibody (Abcam) for 1 h at RT. The arrays were washed three times in PBS-T and then incubated with Alexa Fluor 647–labeled anti–rabbit H+L. Subsequently, the arrays were washed four more times with PBS-T and four times with water before being centrifugally dried (1,000 rpm for 5 min at RT). Finally, the arrays were scanned using a GenePix 4100A Microarray Scanner (Molecular Devices) using the 635-nm channel.

Protein microarray data analysis

Microarray images were gridded and quantitated using GenePix Pro software (version 7; Molecular Devices). Median intensities (features and local backgrounds) were used. Intensity values (feature minus background) from the RhoU-treated and control arrays were used to calculate $M_O = \log_2(\text{RhoU/control})$ and $A = \log_2(\text{sqrt[RhoU*control]})$ values. These values were then Lowess transformed to normalize intensity between arrays and remove technical sources of error (print tip

and location), resulting in the final estimate of magnitude change (M_L). Duplicate features (representing identical protein) were used to calculate the average (Avg M_L) and standard deviation. A *t* test (paired two tailed) was used to assess the statistical significance (p-value) of each estimate (under the null hypothesis that Avg $M_L = 0$). A threshold of 95% confidence ($P < 0.05$) was used to filter data.

Statistical analyses

Datasets were compared using two-tailed *t* tests (unless otherwise stated in the figure legend) and presented as mean ± SEM. Statistical significance was accepted for $P \leq 0.05$.

Online supplemental material

Fig. S1 shows the effect of PAK4 knockdown on MCF-7 cellular adhesion and random migration and confirms that depletion of PAK4 reduces RhoU levels in breast cancer cells. This figure also demonstrates that neither PAK1 nor PAK2 knockdown alters focal adhesion dynamics in MDA-MB-231 cells. Fig. S2 shows that PAK4 can interact with paxillin, vinculin, and RhoV. This figure also shows that RhoU can interact with both PAK1 and PAK4 and that these interactions are through different binding sites. Additionally, this figure highlights that RhoU levels can be regulated by PAK4 and Sharpin overexpression. Fig. S3 shows that RhoU effector loop mutants that still bind PAK4 can rescue the adhesion phenotype of a PAK4 knockdown background. This figure also demonstrates that RhoU is localized in focal adhesions of MDA-MB-231 cells and that levels of paxillin S272 are affected after PAK4, but not PAK1, knockdown. Table S1 lists the RhoU-interacting proteins identified from the protein microarray. Online supplemental material is available at http://www.jcb.org/cgi/content/full/jcb.201501072/DC1.

Acknowledgments

We thank Dr. M. Parsons and Dr. A. Ivetic for critical reading of the manuscript.

C.M. Wells was supported by the Guy's and St. Thomas' Charity. A.E. Dart was supported by the Breast Cancer Campaign (London, England, UK). S.A. Eccles was funded by the Institute of Cancer Research and by Cancer Research UK grant C309/A8274. S.E. Pinder was supported by the Experimental Cancer Medicine Centre and by the National Institute for Health Research Biomedical Research Centre based at Guy's and St. Thomas' National Health Service Foundation Trust and at King's College London. Patient tissue samples were provided by Guy's and St. Thomas' Breast Tissue and Data Bank, which was supported by the Department of Health and the National Institute for Health Research comprehensive Biomedical Research Centre.

The authors declare no competing financial interests.

Submitted: 19 January 2015
Accepted: 14 October 2015

References

Abo, A., J. Qu, M.S. Cammarano, C. Dan, A. Fritsch, V. Baud, B. Belisle, and A. Minden. 1998. PAK4, a novel effector for Cdc42Hs, is implicated in the reorganization of the actin cytoskeleton and in the formation of filopodia. *EMBO J.* 17:6527–6540. http://dx.doi.org/10.1093/emboj/17.22.6527

Ahmed, T., K. Shea, J.R. Masters, G.E. Jones, and C.M. Wells. 2008. A PAK4-LIMK1 pathway drives prostate cancer cell migration downstream of HGF. *Cell. Signal.* 20:1320–1328. http://dx.doi.org/10.1016/j.cellsig.2008.02.021

Baskaran, Y., Y.W. Ng, W. Selamat, F.T. Ling, and E. Manser. 2012. Group I and II mammalian PAKs have different modes of activation by Cdc42. *EMBO Rep.* 13:653–659. http://dx.doi.org/10.1038/embor.2012.75

Bhavsar, P.J., E. Infante, A. Khwaja, and A.J. Ridley. 2013. Analysis of Rho GTPase expression in T-ALL identifies RhoU as a target for Notch involved in T-ALL cell migration. *Oncogene.* 32:198–208. http://dx.doi.org/10.1038/onc.2012.42

Bompard, G., G. Rabeharivelo, M. Frank, J. Cau, C. Delsert, and N. Morin. 2010. Subgroup II PAK-mediated phosphorylation regulates Ran activity during mitosis. *J. Cell Biol.* 190:807–822. http://dx.doi.org/10.1083/jcb.200912056

Callow, M.G., F. Clairvoyant, S. Zhu, B. Schryver, D.B. Whyte, J.R. Bischoff, B. Jallal, and T. Smeal. 2002. Requirement for PAK4 in the anchorage-independent growth of human cancer cell lines. *J. Biol. Chem.* 277:550–558. http://dx.doi.org/10.1074/jbc.M105732200

Chuang, Y.Y., A. Valster, S.J. Coniglio, J.M. Backer, and M. Symons. 2007. The atypical Rho family GTPase Wrch-1 regulates focal adhesion formation and cell migration. *J. Cell Sci.* 120:1927–1934. http://dx.doi.org/10.1242/jcs.03456

Dart, A.E., and C.M. Wells. 2013. P21-activated kinase 4—not just one of the PAK. *Eur. J. Cell Biol.* 92:129–138. http://dx.doi.org/10.1016/j.ejcb.2013.03.002

de la Vega, M., J.F. Burrows, and J.A. Johnston. 2011. Ubiquitination: Added complexity in Ras and Rho family GTPase function. *Small GTPases.* 2:192–201. http://dx.doi.org/10.4161/sgtp.2.4.16707

Dickover, M., J.M. Hegarty, K. Ly, D. Lopez, H. Yang, R. Zhang, N. Tedeschi, T.K. Hsiai, and N.C. Chi. 2014. The atypical Rho GTPase, RhoU, regulates cell-adhesion molecules during cardiac morphogenesis. *Dev. Biol.* 389:182–191. http://dx.doi.org/10.1016/j.ydbio.2014.02.014

Dong, J.M., L.S. Lau, Y.W. Ng, L. Lim, and E. Manser. 2009. Paxillin nuclear-cytoplasmic localization is regulated by phosphorylation of the LD4 motif: evidence that nuclear paxillin promotes cell proliferation. *Biochem. J.* 418:173–184. http://dx.doi.org/10.1042/BJ20080170

Eswaran, J., M. Soundararajan, R. Kumar, and S. Knapp. 2008. UnPAKing the class differences among p21-activated kinases. *Trends Biochem. Sci.* 33:394–403. http://dx.doi.org/10.1016/j.tibs.2008.06.002

Fay, M.J., K.A. Longo, G.A. Karathanasis, D.M. Shope, C.J. Mandernach, J.R. Leong, A. Hicks, K. Pherson, and A. Husain. 2003. Analysis of CUL-5 expression in breast epithelial cells, breast cancer cell lines, normal tissues and tumor tissues. *Mol. Cancer.* 2:40. http://dx.doi.org/10.1186/1476-4598-2-40

Garcia, R., R.A. Franklin, and J.A. McCubrey. 2006. EGF induces cell motility and multi-drug resistance gene expression in breast cancer cells. *Cell Cycle.* 5:2820–2826. http://dx.doi.org/10.4161/cc.5.23.3535

Gnesutta, N., J. Qu, and A. Minden. 2001. The serine/threonine kinase PAK4 prevents caspase activation and protects cells from apoptosis. *J. Biol. Chem.* 276:14414–14419.

Ha, B.H., M.J. Davis, C. Chen, H.J. Lou, J. Gao, R. Zhang, M. Krauthammer, R. Halaban, J. Schlessinger, B.E. Turk, and T.J. Boggon. 2012. Type II p21-activated kinases (PAKs) are regulated by an autoinhibitory pseudosubstrate. *Proc. Natl. Acad. Sci. USA.* 109:16107–16112. http://dx.doi.org/10.1073/pnas.1214447109

Jean, S., and A.A. Kiger. 2012. Coordination between RAB GTPase and phosphoinositide regulation and functions. *Nat. Rev. Mol. Cell Biol.* 13:463–470. http://dx.doi.org/10.1038/nrm3379

Kessler, B.M. 2013. Ubiquitin - omics reveals novel networks and associations with human disease. *Curr. Opin. Chem. Biol.* 17:59–65. http://dx.doi.org/10.1016/j.cbpa.2012.12.024

Kile, B.T., B.A. Schulman, W.S. Alexander, N.A. Nicola, H.M. Martin, and D.J. Hilton. 2002. The SOCS box: a tale of destruction and degradation. *Trends Biochem. Sci.* 27:235–241. http://dx.doi.org/10.1016/S0968-0004(02)02085-6

Kirikoshi, H., H. Sekihara, and M. Katoh. 2001. WNT10A and WNT6, clustered in human chromosome 2q35 region with head-to-tail manner, are strongly coexpressed in SW480 cells. *Biochem. Biophys. Res. Commun.* 283:798–805. http://dx.doi.org/10.1006/bbrc.2001.4855

Lee, R.H., H. Iioka, M. Ohashi, S. Iemura, T. Natsume, and N. Kinoshita. 2007. XRab40 and XCullin5 form a ubiquitin ligase complex essential for the noncanonical Wnt pathway. *EMBO J.* 26:3592–3606. http://dx.doi.org/10.1038/sj.emboj.7601781

Li, X., and A. Minden. 2005. PAK4 functions in tumor necrosis factor (TNF) α-induced survival pathways by facilitating TRADD binding to the TNF receptor. *J. Biol. Chem.* 280:41192–41200. http://dx.doi.org/10.1074/jbc.M506884200

Li, Y., Y. Shao, Y. Tong, T. Shen, J. Zhang, Y. Li, H. Gu, and F. Li. 2012. Nucleo-cytoplasmic shuttling of PAK4 modulates β-catenin intracellular

translocation and signaling. *Biochim. Biophys. Acta.* 1823:465–475. http://dx.doi.org/10.1016/j.bbamcr.2011.11.013

Liu, Y., H. Xiao, Y. Tian, T. Nekrasova, X. Hao, H.J. Lee, N. Suh, C.S. Yang, and A. Minden. 2008. The pak4 protein kinase plays a key role in cell survival and tumorigenesis in athymic mice. *Mol. Cancer Res.* 6:1215–1224. http://dx.doi.org/10.1158/1541-7786.MCR-08-0087

Liu, Y., N. Chen, X. Cui, X. Zheng, L. Deng, S. Price, V. Karantza, and A. Minden. 2010. The protein kinase Pak4 disrupts mammary acinar architecture and promotes mammary tumorigenesis. *Oncogene.* 29:5883–5894. http://dx.doi.org/10.1038/onc.2010.329

Murray, B.W., C. Guo, J. Piraino, J.K. Westwick, C. Zhang, J. Lamerdin, E. Dagostino, D. Knighton, C.M. Loi, M. Zager, et al. 2010. Small-molecule p21-activated kinase inhibitor PF-3758309 is a potent inhibitor of oncogenic signaling and tumor growth. *Proc. Natl. Acad. Sci. USA.* 107:9446–9451. http://dx.doi.org/10.1073/pnas.0911863107

Nayal, A., D.J. Webb, C.M. Brown, E.M. Schaefer, M. Vicente-Manzanares, and A.R. Horwitz. 2006. Paxillin phosphorylation at Ser273 localizes a GIT1-PIX-PAK complex and regulates adhesion and protrusion dynamics. *J. Cell Biol.* 173:587–589. http://dx.doi.org/10.1083/jcb.200509075

Nethe, M., and P.L. Hordijk. 2010. The role of ubiquitylation and degradation in RhoGTPase signalling. *J. Cell Sci.* 123:4011–4018. http://dx.doi.org/10.1242/jcs.078360

Nethe, M., E.C. Anthony, M. Fernandez-Borja, R. Dee, D. Geerts, P.J. Hensbergen, A.M. Deelder, G. Schmidt, and P.L. Hordijk. 2010. Focal-adhesion targeting links caveolin-1 to a Rac1-degradation pathway. *J. Cell Sci.* 123:1948–1958. http://dx.doi.org/10.1242/jcs.062919

Neve, R.M., K. Chin, J. Fridlyand, J. Yeh, F.L. Baehner, T. Fevr, L. Clark, N. Bayani, J.P. Coppe, F. Tong, et al. 2006. A collection of breast cancer cell lines for the study of functionally distinct cancer subtypes. *Cancer Cell.* 10:515–527. http://dx.doi.org/10.1016/j.ccr.2006.10.008

Omura, S., Y. Sasaki, Y. Iwai, and H. Takeshima. 1995. Staurosporine, a potentially important gift from a microorganism. *J. Antibiot.* 48:535–548. http://dx.doi.org/10.7164/antibiotics.48.535

Ory, S., H. Brazier, and A. Blangy. 2007. Identification of a bipartite focal adhesion localization signal in RhoU/Wrch-1, a Rho family GTPase that regulates cell adhesion and migration. *Biol. Cell.* 99:701–716. http://dx.doi.org/10.1042/BC20070058

Park, M.H., H.S. Lee, C.S. Lee, S.T. You, D.J. Kim, B.H. Park, M.J. Kang, W.D. Heo, E.Y. Shin, M.A. Schwartz, and E.G. Kim. 2013. p21-Activated kinase 4 promotes prostate cancer progression through CREB. *Oncogene.* 32:2475–2482. http://dx.doi.org/10.1038/onc.2012.255

Qu, J., X. Li, B.G. Novitch, Y. Zheng, M. Kohn, J.M. Xie, S. Kozinn, R. Bronson, A.A. Beg, and A. Minden. 2003. PAK4 kinase is essential for embryonic viability and for proper neuronal development. *Mol. Cell. Biol.* 23:7122–7133. http://dx.doi.org/10.1128/MCB.23.20.7122-7133.2003

Rafn, B., C.F. Nielsen, S.H. Andersen, P. Szyniarowski, E. Corcelle-Termeau, E. Valo, N. Fehrenbacher, C.J. Olsen, M. Daugaard, C. Egebjerg, et al. 2012. ErbB2-driven breast cancer cell invasion depends on a complex signaling network activating myeloid zinc finger-1-dependent cathepsin B expression. *Mol. Cell.* 45:764–776. http://dx.doi.org/10.1016/j.molcel.2012.01.029

Rantala, J.K., J. Pouwels, T. Pellinen, S. Veltel, P. Laasola, E. Mattila, C.S. Potter, T. Duffy, J.P. Sundberg, O. Kallioniemi, et al. 2011. SHARPIN is an endogenous inhibitor of β1-integrin activation. *Nat. Cell Biol.* 13:1315–1324. http://dx.doi.org/10.1038/ncb2340

Rodriguez, M.S., J.M. Desterro, S. Lain, D.P. Lane, and R.T. Hay. 2000. Multiple C-terminal lysine residues target p53 for ubiquitin-proteasome-mediated degradation. *Mol. Cell. Biol.* 20:8458–8467. http://dx.doi.org/10.1128/MCB.20.22.8458-8467.2000

Rolli-Derkinderen, M., V. Sauzeau, L. Boyer, E. Lemichez, C. Baron, D. Henrion, G. Loirand, and P. Pacaud. 2005. Phosphorylation of serine 188 protects RhoA from ubiquitin/proteasome-mediated degradation in vascular smooth muscle cells. *Circ. Res.* 96:1152–1160. http://dx.doi.org/10.1161/01.RES.0000170084.88780.ea

Saras, J., P. Wollberg, and P. Aspenström. 2004. Wrch1 is a GTPase-deficient Cdc42-like protein with unusual binding characteristics and cellular effects. *Exp. Cell Res.* 299:356–369. http://dx.doi.org/10.1016/j.yexcr.2004.05.029

Schiavone, D., S. Dewilde, F. Vallania, J. Turkson, F. Di Cunto, and V. Poli. 2009. The RhoU/Wrch1 Rho GTPase gene is a common transcriptional target of both the gp130/STAT3 and Wnt-1 pathways. *Biochem. J.* 421:283–292. http://dx.doi.org/10.1042/BJ20090061

Shepelev, M.V., and I.V. Korobko. 2012. Pak6 protein kinase is a novel effector of an atypical Rho family GTPase Chp/RhoV. *Biochemistry Mosc.* 77:26–32. http://dx.doi.org/10.1134/S0006297912010038

Shutes, A., A.C. Berzat, A.D. Cox, and C.J. Der. 2004. Atypical mechanism of regulation of the Wrch-1 Rho family small GTPase. *Curr. Biol.* 14:2052–2056. http://dx.doi.org/10.1016/j.cub.2004.11.011

Siu, M.K., H.Y. Chan, D.S. Kong, E.S. Wong, O.G. Wong, H.Y. Ngan, K.F. Tam, H. Zhang, Z. Li, Q.K. Chan, et al. 2010. p21-activated kinase 4 regulates ovarian cancer cell proliferation, migration, and invasion and contributes to poor prognosis in patients. *Proc. Natl. Acad. Sci. USA.* 107:18622–18627. http://dx.doi.org/10.1073/pnas.0907481107

Tabusa, H., T. Brooks, and A.J. Massey. 2013. Knockdown of PAK4 or PAK1 inhibits the proliferation of mutant KRAS colon cancer cells independently of RAF/MEK/ERK and PI3K/AKT signaling. *Mol. Cancer Res.* 11:109–121. http://dx.doi.org/10.1158/1541-7786.MCR-12-0466

Tao, W., D. Pennica, L. Xu, R.F. Kalejta, and A.J. Levine. 2001. Wrch-1, a novel member of the Rho gene family that is regulated by Wnt-1. *Genes Dev.* 15:1796–1807. http://dx.doi.org/10.1101/gad.894301

Teckchandani, A., G.S. Laszlo, S. Simó, K. Shah, C. Pilling, A.A. Strait, and J.A. Cooper. 2014. Cullin 5 destabilizes Cas to inhibit Src-dependent cell transformation. *J. Cell Sci.* 127:509–520. http://dx.doi.org/10.1242/jcs.127829

Tong, D., K. Czerwenka, J. Sedlak, C. Schneeberger, I. Schiebel, N. Concin, S. Leodolter, and R. Zeillinger. 1999. Association of in vitro invasiveness and gene expression of estrogen receptor, progesterone receptor, pS2 and plasminogen activator inhibitor-1 in human breast cancer cell lines. *Breast Cancer Res. Treat.* 56:91–97. http://dx.doi.org/10.1023/A:1006262501062

Vignal, E., M. De Toledo, F. Comunale, A. Ladopoulou, C. Gauthier-Rouvière, A. Blangy, and P. Fort. 2000. Characterization of TCL, a new GTPase of the rho family related to TC10 and Cdc42. *J. Biol. Chem.* 275:36457–36464. http://dx.doi.org/10.1074/jbc.M003487200

Visvikis, O., P. Lorès, L. Boyer, P. Chardin, E. Lemichez, and G. Gacon. 2008. Activated Rac1, but not the tumorigenic variant Rac1b, is ubiquitinated on Lys 147 through a JNK-regulated process. *FEBS J.* 275:386–396. http://dx.doi.org/10.1111/j.1742-4658.2007.06209.x

Wagner, S.A., P. Beli, B.T. Weinert, C. Schölz, C.D. Kelstrup, C. Young, M.L. Nielsen, J.V. Olsen, C. Brakebusch, and C. Choudhary. 2012. Proteomic analyses reveal divergent ubiquitylation site patterns in murine tissues. *Mol. Cell. Proteomics.* 11:1578–1585. http://dx.doi.org/10.1074/mcp.M112.017905

Wallace, S.W., J. Durgan, D. Jin, and A. Hall. 2010. Cdc42 regulates apical junction formation in human bronchial epithelial cells through PAK4 and Par6B. *Mol. Biol. Cell.* 21:2996–3006. http://dx.doi.org/10.1091/mbc.E10-05-0429

Wang, G., Y. Gao, L. Li, G. Jin, Z. Cai, J.I. Chao, and H.K. Lin. 2012. K63-linked ubiquitination in kinase activation and cancer. *Front Oncol.* 2:5. http://dx.doi.org/10.3389/fonc.2012.00005

Wang, W., L. Lim, Y. Baskaran, E. Manser, and J. Song. 2013. NMR binding and crystal structure reveal that intrinsically-unstructured regulatory domain auto-inhibits PAK4 by a mechanism different from that of PAK1. *Biochem. Biophys. Res. Commun.* 438:169–174. http://dx.doi.org/10.1016/j.bbrc.2013.07.047

Wehrle-Haller, B. 2012. Structure and function of focal adhesions. *Curr. Opin. Cell Biol.* 24:116–124. http://dx.doi.org/10.1016/j.ceb.2011.11.001

Weissman, A.M. 2001. Themes and variations on ubiquitylation. *Nat. Rev. Mol. Cell Biol.* 2:169–178. http://dx.doi.org/10.1038/35056563

Wells, C.M., A. Abo, and A.J. Ridley. 2002. PAK4 is activated via PI3K in HGF-stimulated epithelial cells. *J. Cell Sci.* 115:3947–3956. http://dx.doi.org/10.1242/jcs.00080

Wells, C.M., A.D. Whale, M. Parsons, J.R. Masters, and G.E. Jones. 2010. PAK4: a pluripotent kinase that regulates prostate cancer cell adhesion. *J. Cell Sci.* 123:1663–1673. http://dx.doi.org/10.1242/jcs.055707

Whale, A.D., A. Dart, M. Holt, G.E. Jones, and C.M. Wells. 2013. PAK4 kinase activity and somatic mutation promote carcinoma cell motility and influence inhibitor sensitivity. *Oncogene.* 32:2114–2120. http://dx.doi.org/10.1038/onc.2012.233

Wilson, E., K. Leszczynska, N.S. Poulter, F. Edelmann, V.A. Salisbury, P.J. Noy, A. Bacon, J.Z. Rappoport, J.K. Heath, R. Bicknell, and V.L. Heath. 2014. RhoJ interacts with the GIT–PIX complex and regulates focal adhesion disassembly. *J. Cell Sci.* 127:3039–3051. http://dx.doi.org/10.1242/jcs.140434

Wu, X., and J.A. Frost. 2006. Multiple Rho proteins regulate the subcellular targeting of PAK5. *Biochem. Biophys. Res. Commun.* 351:328–335. http://dx.doi.org/10.1016/j.bbrc.2006.09.172

Yu, W., Y. Kanaan, Y.K. Bae, and E. Gabrielson. 2009. Chromosomal changes in aggressive breast cancers with basal-like features. *Cancer Genet. Cytogenet.* 193:29–37. http://dx.doi.org/10.1016/j.cancergencyto.2009.03.017

Zhang, H.J., M.K. Siu, M.C. Yeung, L.L. Jiang, V.C. Mak, H.Y. Ngan, O.G. Wong, H.Q. Zhang, and A.N. Cheung. 2011. Overexpressed PAK4 promotes proliferation, migration and invasion of choriocarcinoma. *Carcinogenesis.* 32:765–771. http://dx.doi.org/10.1093/carcin/bgr033

Zhang, J., J. Wang, Q. Guo, Y. Wang, Y. Zhou, H. Peng, M. Cheng, D. Zhao, and F. Li. 2012. LCH-7749944, a novel and potent p21-activated kinase 4 inhibitor, suppresses proliferation and invasion in human gastric cancer cells. *Cancer Lett.* 317:24–32. http://dx.doi.org/10.1016/j.canlet.2011.11.007